REPORT T-157 FEBRUARY, 1985

CSL COORDINATED SCIENCE LABORATORY

NONLINEAR SOLUTIONS OF THE WIGLEY HULL

R. R. REYES
S. M. YEN

UNIVERSITY OF ILLINOIS AT URBANA-CHAMPAIGN

REPORT DOCUMENTATION PAGE

1a. REPORT SECURITY CLASSIFICATION Unclassified	1b. RESTRICTIVE MARKINGS None
2a. SECURITY CLASSIFICATION AUTHORITY N/A 2b. DECLASSIFICATION/DOWNGRADING SCHEDULE N/A	3. DISTRIBUTION/AVAILABILITY OF REPORT Approved for public release, distribution unlimited.
4. PERFORMING ORGANIZATION REPORT NUMBER(S) T-157	5. MONITORING ORGANIZATION REPORT NUMBER(S) N/A
6a. NAME OF PERFORMING ORGANIZATION Coordinated Science Lab. Univ. of Illinois 6b. OFFICE SYMBOL (If applicable) N/A	7a. NAME OF MONITORING ORGANIZATION Office of Naval Research
6c. ADDRESS (City, State and ZIP Code) 1101 W. Springfield Avenue Urbana, Illinois 61801	7b. ADDRESS (City, State and ZIP Code) 800 N. Quincy Street Arlington, VA 22217
8a. NAME OF FUNDING/SPONSORING ORGANIZATION Office of Naval Research 8b. OFFICE SYMBOL (If applicable)	9. PROCUREMENT INSTRUMENT IDENTIFICATION NUMBER Contract #N00014-80-C-0740 (NR334-004)
8c. ADDRESS (City, State and ZIP Code) 800 N. Quincy Street Arlington, VA 22217	10. SOURCE OF FUNDING NOS. PROGRAM ELEMENT NO.: N/A; PROJECT NO.: N/A; TASK NO.: N/A; WORK UNIT NO.: N/A
11. TITLE (Include Security Classification) Nonlinear Solutions of the Wigley Hull	

12. PERSONAL AUTHOR(S)
R. R. Reyes and S. M. Yen

13a. TYPE OF REPORT	13b. TIME COVERED	14. DATE OF REPORT (Yr., Mo., Day)	15. PAGE COUNT
Technical	FROM ________ TO ________	February, 1985	38

16. SUPPLEMENTARY NOTATION
N/A

17. COSATI CODES			18. SUBJECT TERMS (Continue on reverse if necessary and identify by block number)
FIELD	GROUP	SUB. GR.	Nonlinear ship wave, wave resistance, Wigley hull, Numerical solution, finite difference method.

19. ABSTRACT (Continue on reverse if necessary and identify by block number)

Nonlinear solutions for the Wigley hull for Foude numbers = 0.200, 0.224, 0.233, 0.266, 0.280, 0.308 and 0.329 are presented in this report.

20. DISTRIBUTION/AVAILABILITY OF ABSTRACT	21. ABSTRACT SECURITY CLASSIFICATION
UNCLASSIFIED/UNLIMITED ☒ SAME AS RPT. ☐ DTIC USERS ☐	Unclassified

22a. NAME OF RESPONSIBLE INDIVIDUAL	22b. TELEPHONE NUMBER (Include Area Code)	22c. OFFICE SYMBOL
		None

DD FORM 1473, 83 APR — EDITION OF 1 JAN 73 IS OBSOLETE.

SECURITY CLASSIFICATION OF THIS PAGE

TABLE OF CONTENTS

CHAPTER I

INTRODUCTION

A numerical method has been developed to solve the nonlinear ship wave problem [1] and solutions have been obtained for the Wigley hull for the linearized, thin ship problem, the Neumann-Kelvin problem and the nonlinear ship wave problem [1]. Additional solutions have been obtained for the nonlinear ship wave problem and are presented in this report.

CHAPTER II

NONLINEAR SOLUTIONS

Attempts were made to obtain solutions for Fr = 0.200, 0.224, 0.233, 0.266, 0.280, 0.308 and 0.329. The convergence level of each solution is obtained by increasing successively the parameter IC. This parameter controls the number of iterations performed on the free surface at each time step. The number of iterations is equal to (IC-1); therefore, an IC value of one corresponds to solving the Neumann-Kelvin problem. To check the convergence level, the partial residual is calculated for each iteration. It is a measure of the accuracy of implementation of the free surface conditions. To obtain the partial residual, the residual which is equal to $\nabla^2\phi$ is first calculated for mesh points adjacent to the free surface, except those on all the boundaries and those adjacent to the hull. Then, the sum of the square of the residuals and its square root are evaluated after each iteration. For a fixed number of iterations, the partial residual obtained at the final iteration grows with time, since the wave height grows in time. The maximum partial residual obtained during the period of calculation is used to monitor the convergence level. This partial residual decreases as IC increases, since more iterations are performed on the free surface to implement the free surface conditions. As solutions are obtained for a larger value of IC, the free surface conditions are successively better approximated.

Sixteen runs have been made. The results are summarized in Table 2.1, which gives the IC value, the maximum partial residual and the wave resistance coefficient C_w for each case. The partial residuals obtained for solutions with Fr = 0.200, 0.224 and 0.233 are 10^{-5} for 0.200 and 0.224, and 10^{-4}

Table 2.1

RUN	Fr	IC	Partial Residual	C_w
1	0.200	2	10^{-2}	0.59
2	0.200	4	10^{-4}	0.59
3	0.200	6	10^{-5}	0.59
4	0.224	2	10^{-1}	0.80
5	0.224	4	10^{-3}	0.71
6	0.224	6	10^{-5}	0.70
7	0.233	2	10^{-1}	1.16
8	0.233	4	10^{-3}	1.06
9	0.233	6	10^{-4}	1.06
10	0.266	2	10^{0}	1.70
11	0.266	4	10^{-1}	1.72
12	0.280	2	10^{0}	1.67
13	0.280	4	10^{-1}	1.67
14	0.308	2	10^{0}	1.88
15	0.308	4	10^{-1}	1.78
16	0.329	2	10^{0}	2.22

for 0.233. These values were obtained at an IC value of six, i.e., five iterations done on the free surface. Figures 2.1 - 2.3 show the steady state, wave height profiles along the ship hull for IC = 2, 4 and 6. We observe that the difference in the wave profiles is insignificant between the case with IC = 4 and that with IC = 6. These results confirm that the solutions for the three Froude numbers converge as more iterations are used to implement the free surface boundary conditions.

The lowest partial residual obtained for solutions for Fr = 0.266, 0.280 and 0.308 is 10^{-1} at an IC value of four. For the Froude number 0.329, the lower partial residual obtained is 10^{0} at an IC value of two. The hull wave profiles for Fr = 0.266, 0.280, 0.308 and 0.329 are shown in Figures 2.4 - 2.7.

As seen in Table 2.1, the influence of the parameter IC on the wave resistance is very small. Figure 2.8 compares the calculations of C_w as a function of Fr for the nonlinear problem, the Neumann-Kelvin problem and the linear problem.

It would be of interest to study the evolution of the surface wave profile in the entire computational domain. The profile exhibits not only the nature of the solution but also errors that may exist. Figure 2.9 shows the evolution of surface waves for Fr = 0.200 for T=1-9. For each value of T, wave profiles are shown in two different view angles. At T = 8, we observe that two grid interval waves start to occur at the upstream corner of the domain. These disturbances then propagate downstream. Attempts have been made to remove these disturbances by filtering, using a zeroth-order scheme [2]. It was applied at every time step to the wave heights in a region at the front of the domain as shown in Figure 2.10. The finite difference scheme applied on the interior mesh points of this region is given by

$$\bar{\eta}_{i,j} = (\eta_{i,j+1} + \eta_{i,j-1}) / 4 + \eta_{i,j}/2 \ , \qquad (2.1)$$

where

$$1 < i < 5 \quad , \quad 2 < j < 32 \ .$$

For the mesh points that lie on the symmetry and far field boundaries (J=1 and J=33), the following alternate form of Eq. (2.1) was used

$$\bar{\eta}_{i,j} = [\eta_{i,j+1} + \eta_{i,j}] / 2. \qquad (2.2)$$

The result of applying this filtering technique is shown in Figures 2.11 and 2.12. Figure 2.11 shows two surface waves at T=9, one with filtering and the other without. The result with filtering shows that the upstream region is free of any disturbances. Figure 2.12 shows the wave height profiles along the ship hull for the two cases. Since the two wave profiles are in agreement, we conclude that the disturbances do not affect the solution near the hull surface.

Figures 2.13 - 2.15 show a comparison of the surface wave profiles of the Linear problem, the Neumann-Kelvin problem and the nonlinear problem for Fr = 0.266. The wave patterns for each of these cases are shown at T=3, T=6 and T=9. Figures 2.16 - 2.20 show the steady state wave patterns at T=9 for the Fr = 0.224, 0.233, 0.280, 0.308 and 0.329, respectively. These surface wave profiles also show that our method of implementation of the open boundary condition is successful in that no significant waves are seen to reflect from the downstream boundary.

REFERENCES

1. Chamberlain, R. R. and Yen, S. M., "Numerical Solution of the Nonlinear Ship Wave Problem," Report T-150, Coordinated Science Laboratory, University of Illinois, January 1985.

2. Hall, D. R., "Numerical Solutions of Nonlinear Free Surface Wave Problems," Ph.D. Thesis, University of Illinois, Urbana, IL, 1984.

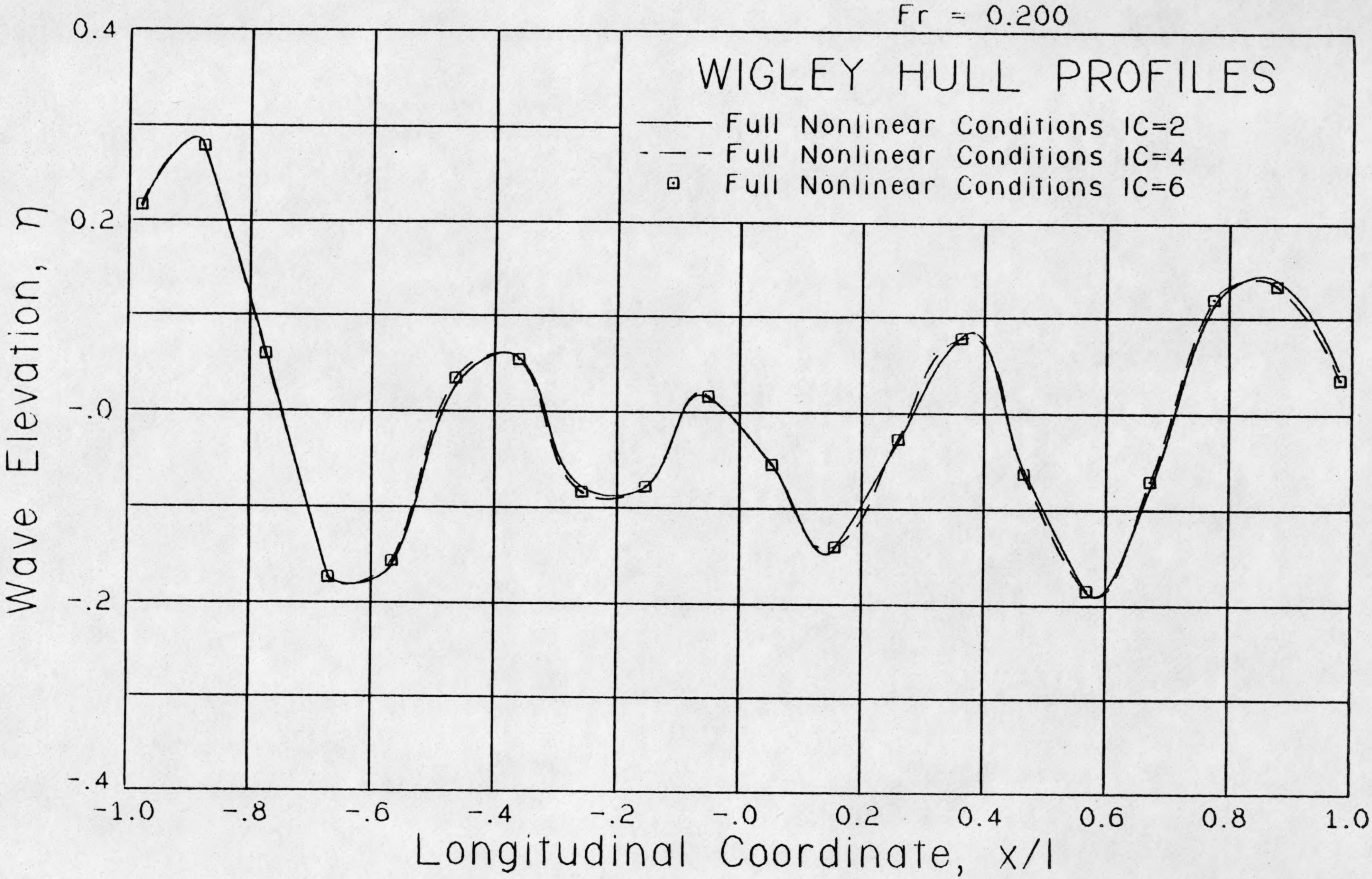

Figure 2.1 Comparison of the Wigley hull wave profiles for Fr=0.200 and IC= to 2, 4 and 6.

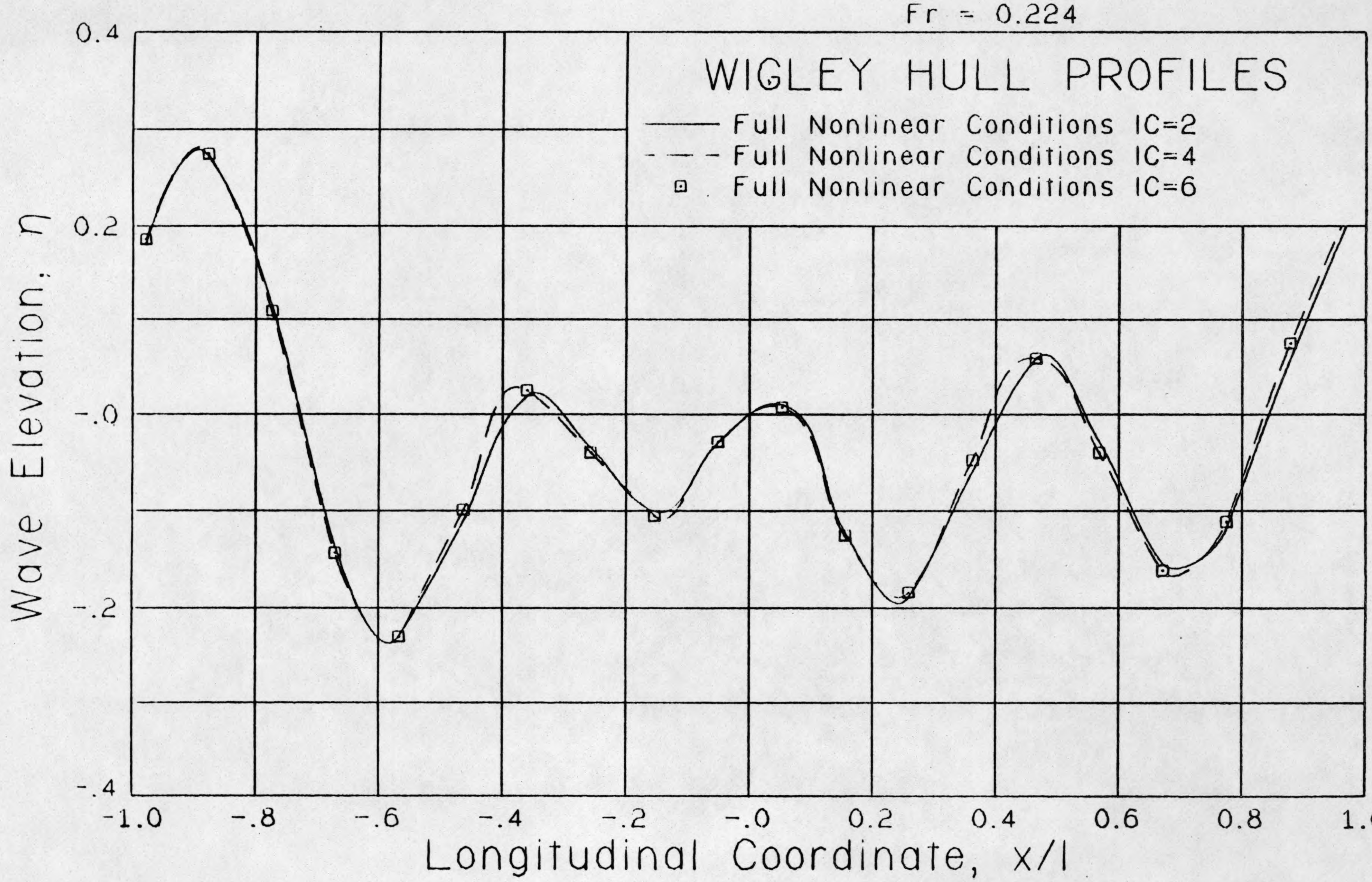

Figure 2.2 Comparison of the Wigley hull wave profiles for Fr=0.224 and IC= to 2, 4 and 6.

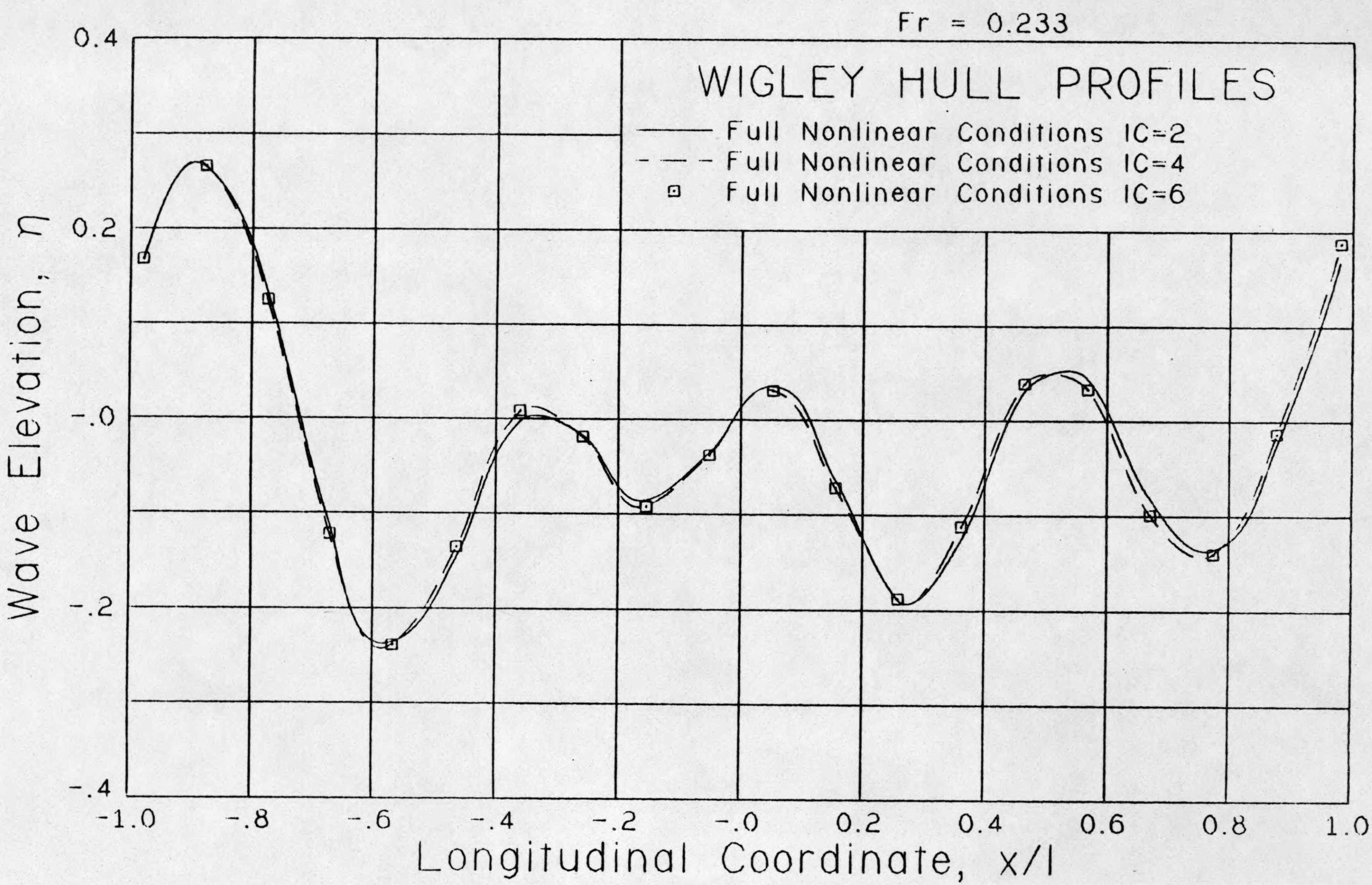

Figure 2.3 Comparison of the Wigley hull wave profiles for Fr=0.233 and IC= to 2, 4 and 6.

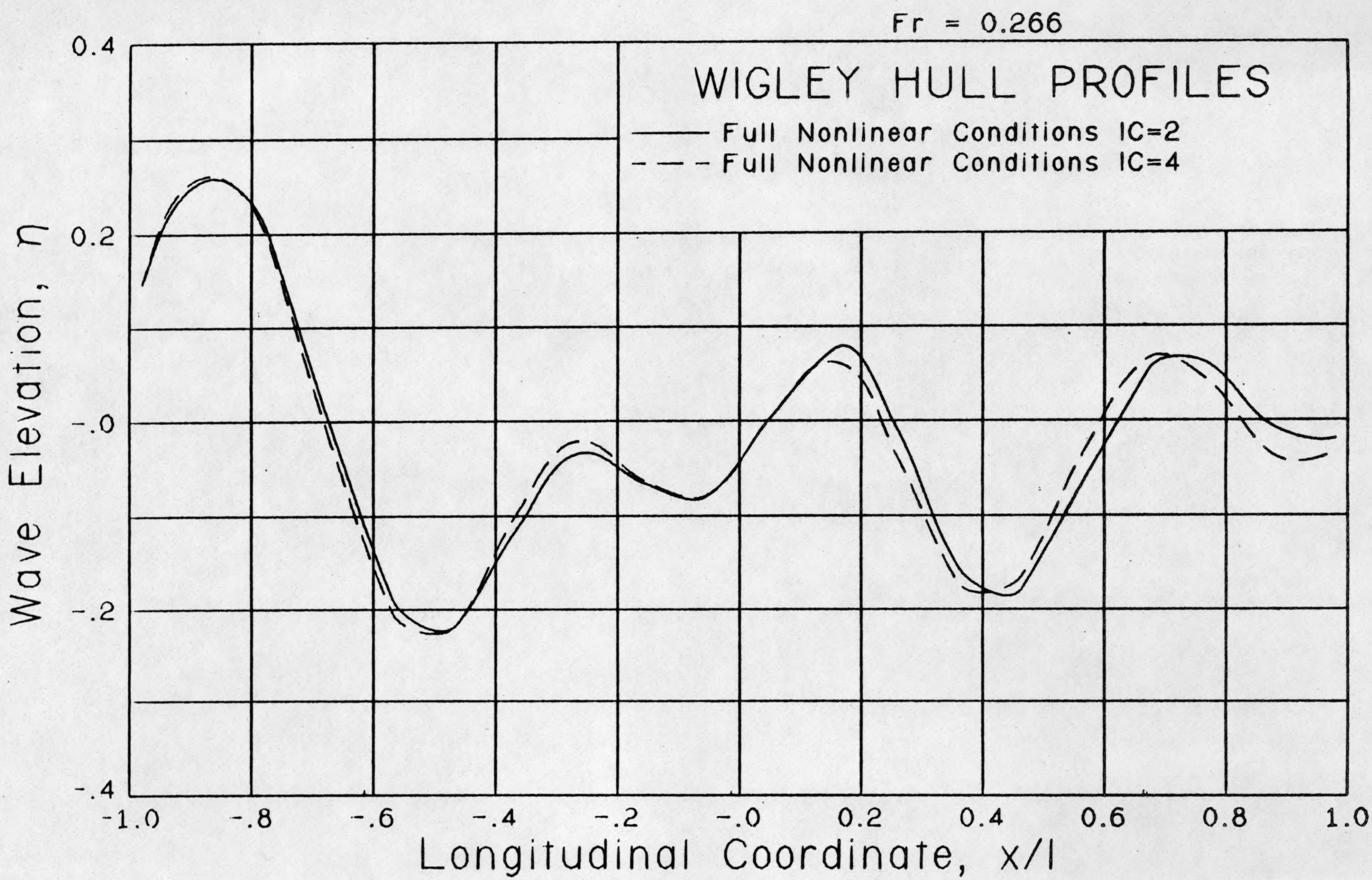

Figure 2.4 Comparison of the Wigley hull wave profiles for Fr=0.266 and IC= to 2 and 4.

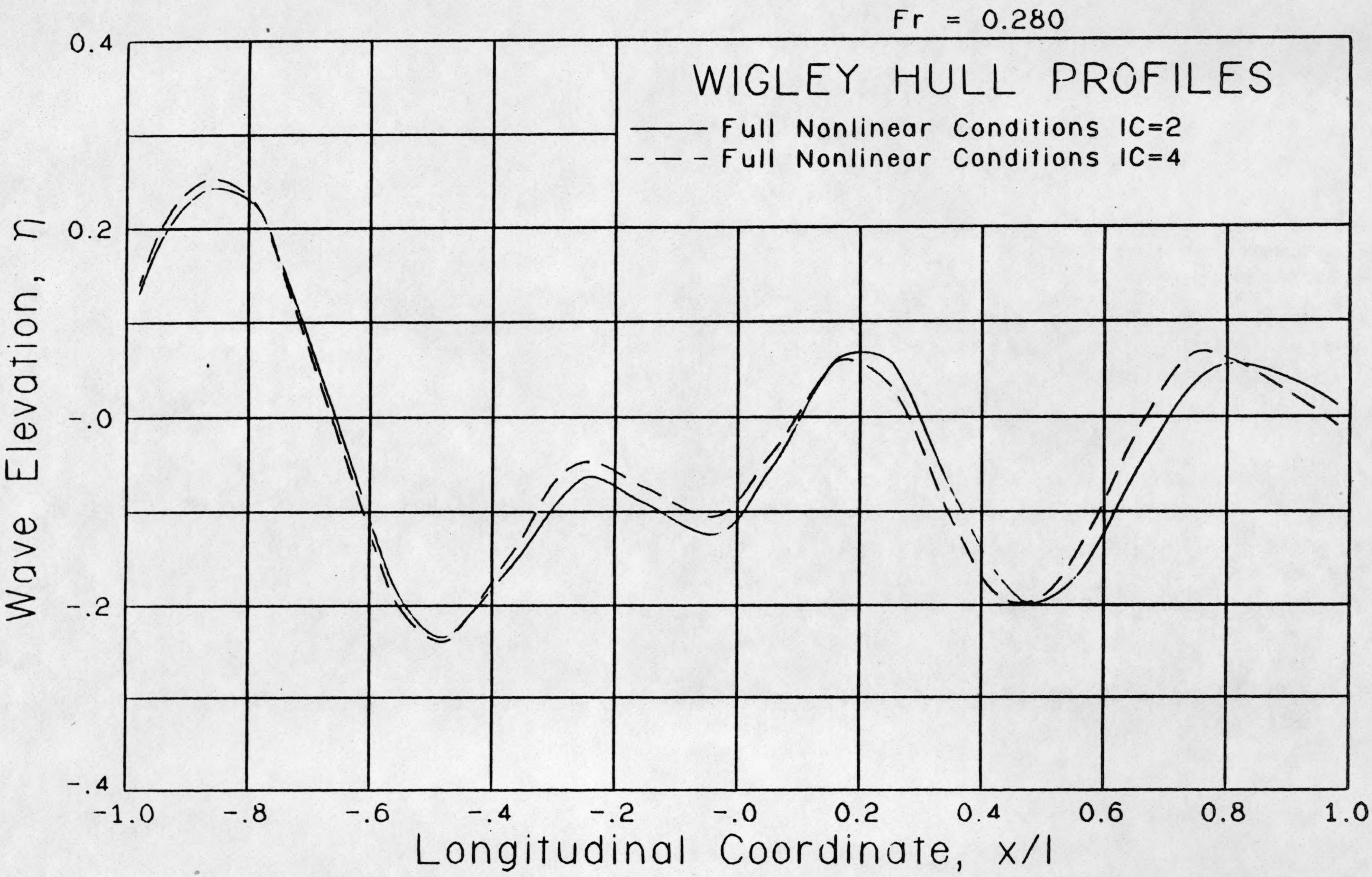

Figure 2.5 Comparison of the Wigley hull wave profiles for Fr=0.280 and IC= to 2 and 4.

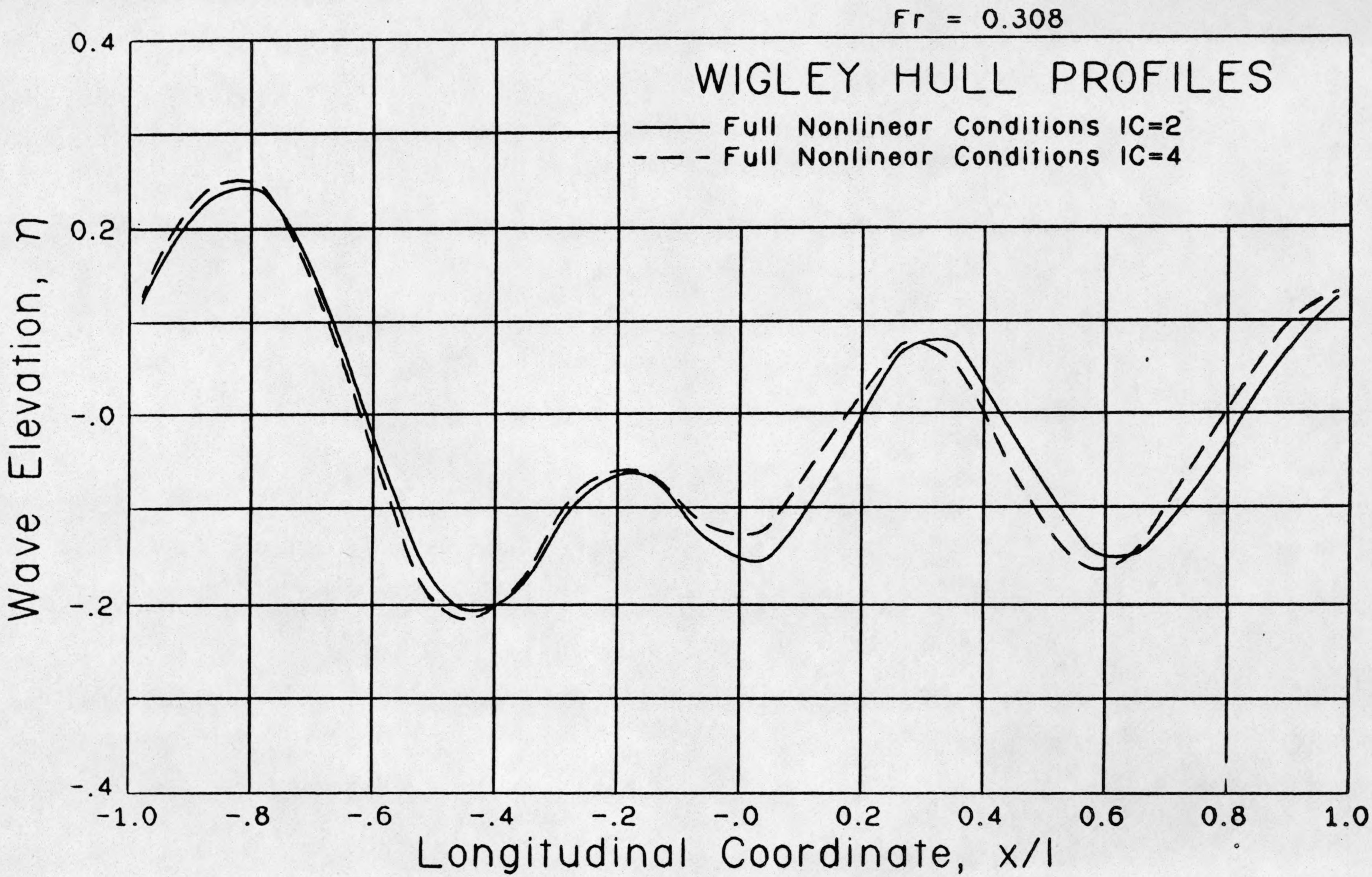

Figure 2.6 Comparison of the Wigley hull wave profiles for Fr=0.308 and IC= to 2 and 4.

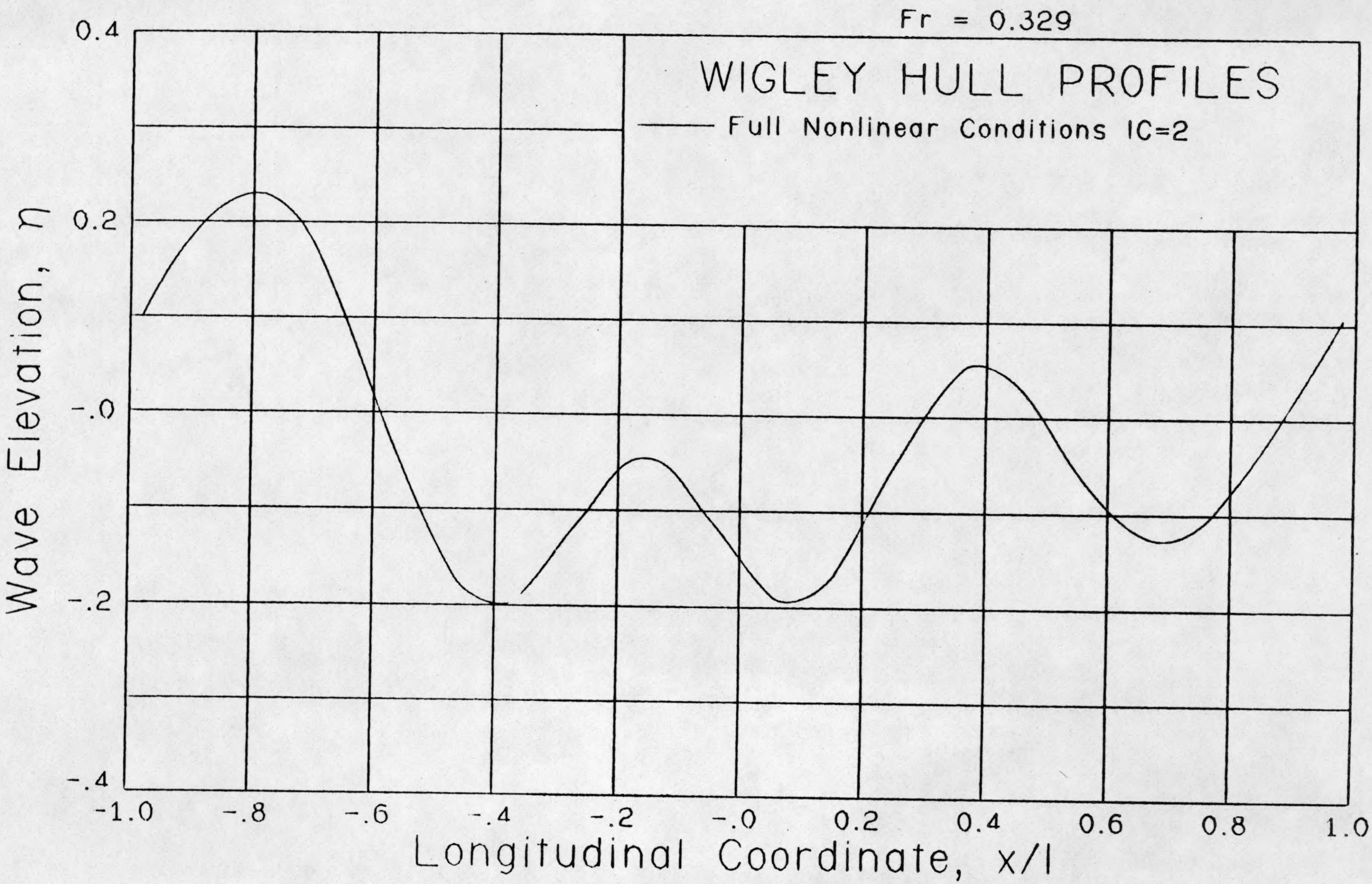

Figure 2.7 Wigley hull wave profile for Fr=0.329 and IC=2.

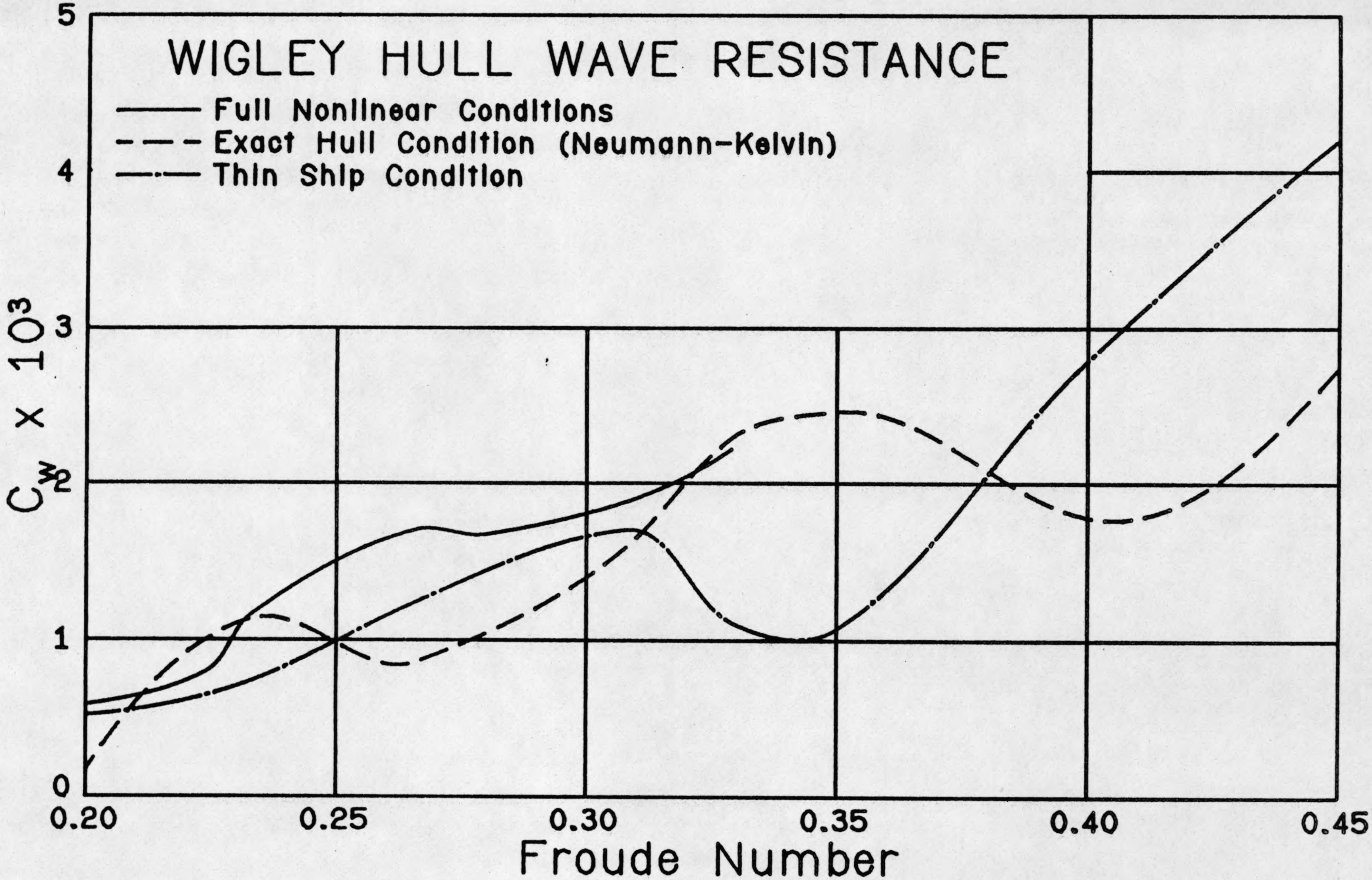

Figure 2.8 Comparison of the Wigley hull wave resistance vs. Froude number for the full nonlinear conditions, the exact hull condition and the thin ship condition.

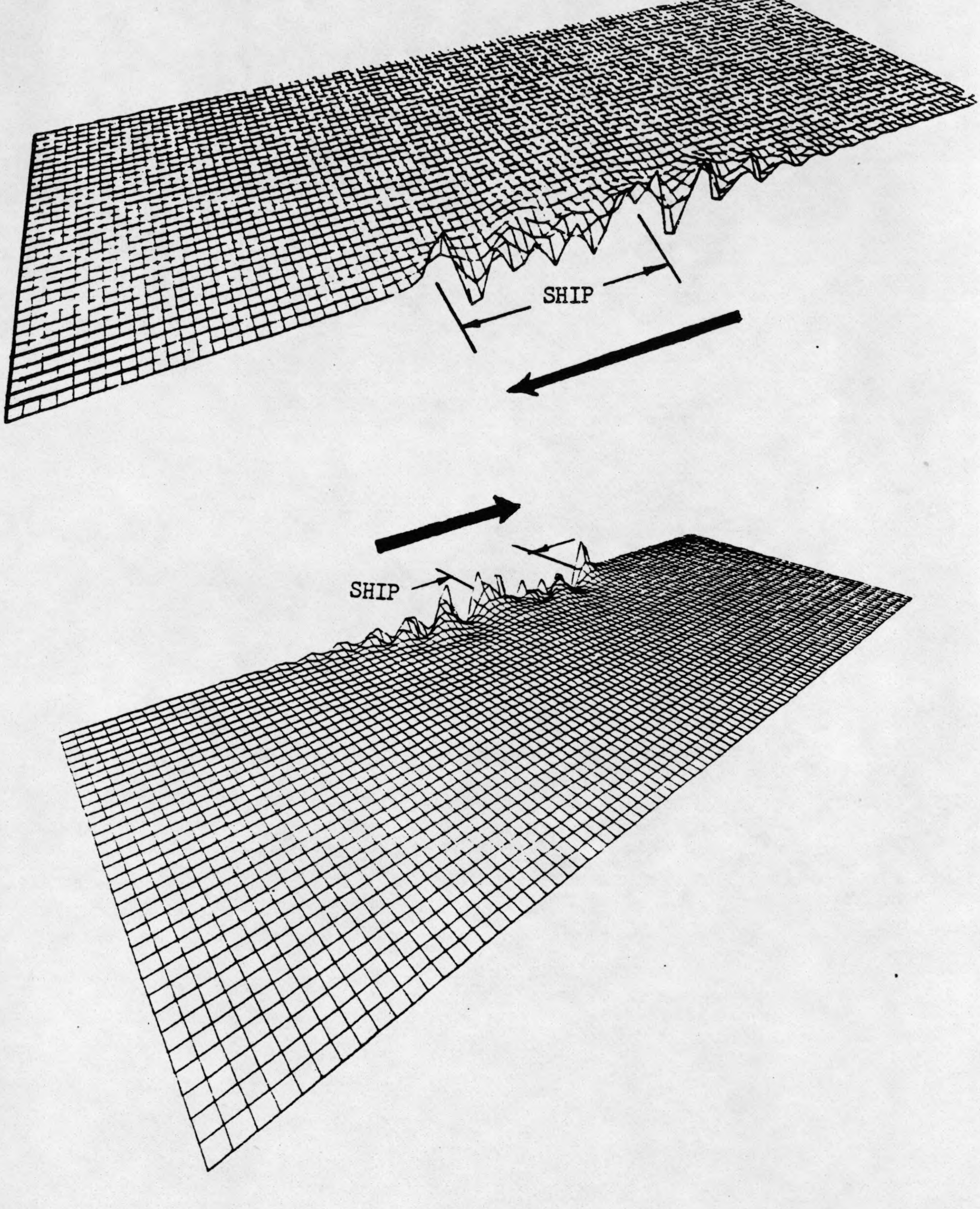

Figure 2.9a Two views of the free surface waves at T=1 for Fr=0.200(Waveheight nondimensionalized by $Fr^2/2$).

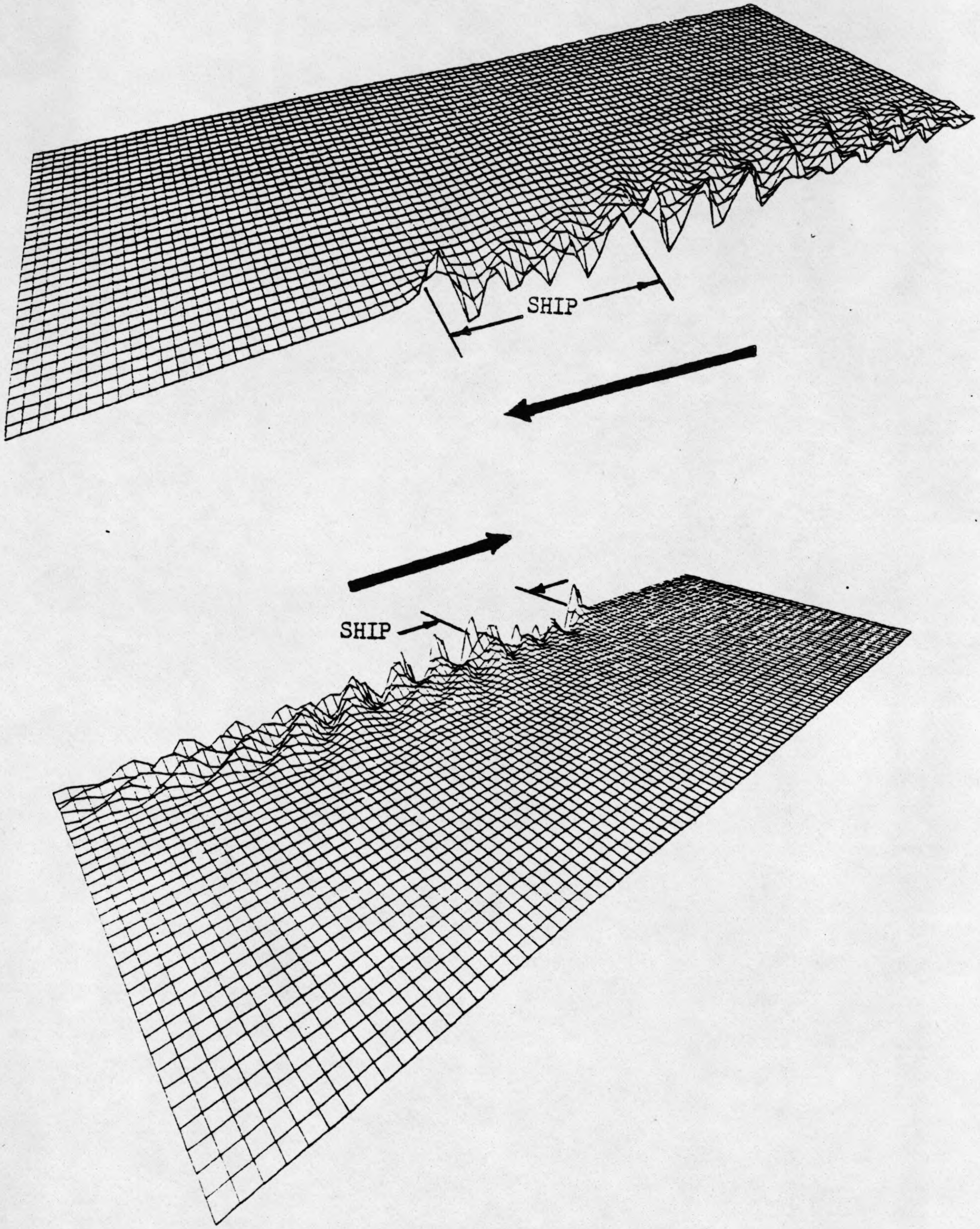

Figure 2.9b Two views of the free surface waves at T=2 for Fr=0.200.

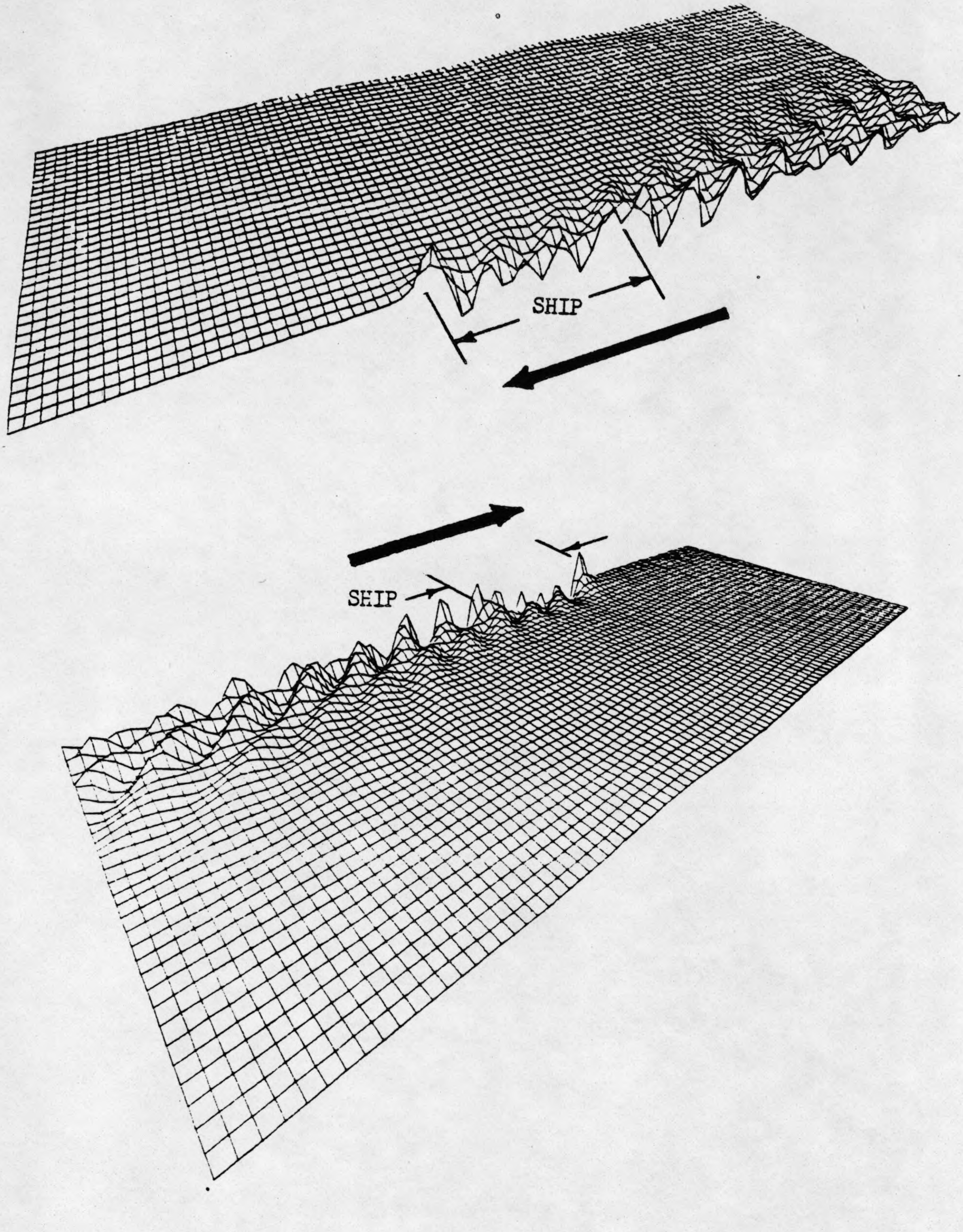

Figure 2.9c Two views of the free surface waves at T=3 for Fr=0.200.

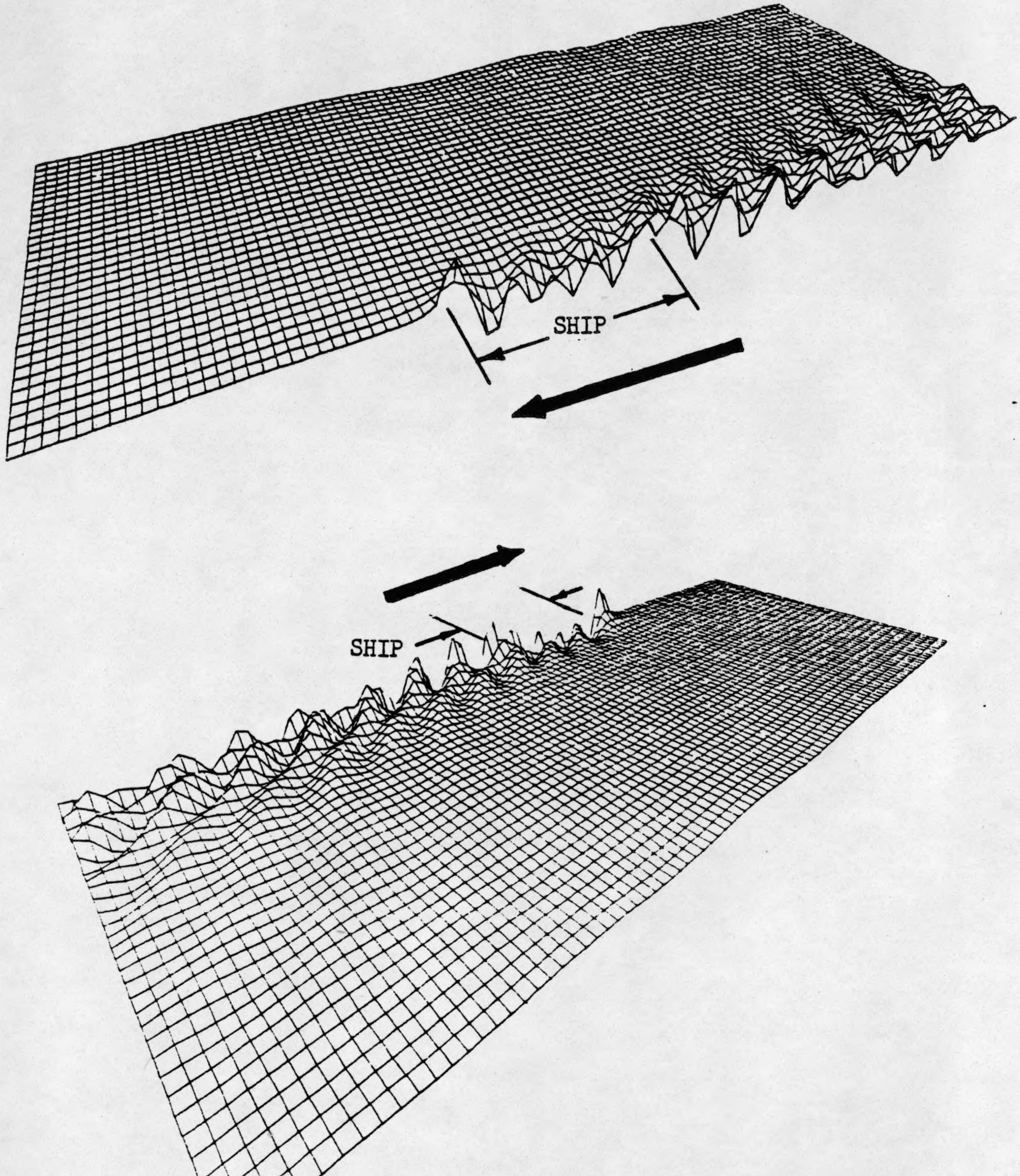

Figure 2.9d Two views of the free surface waves at T=4 for Fr=0.200.

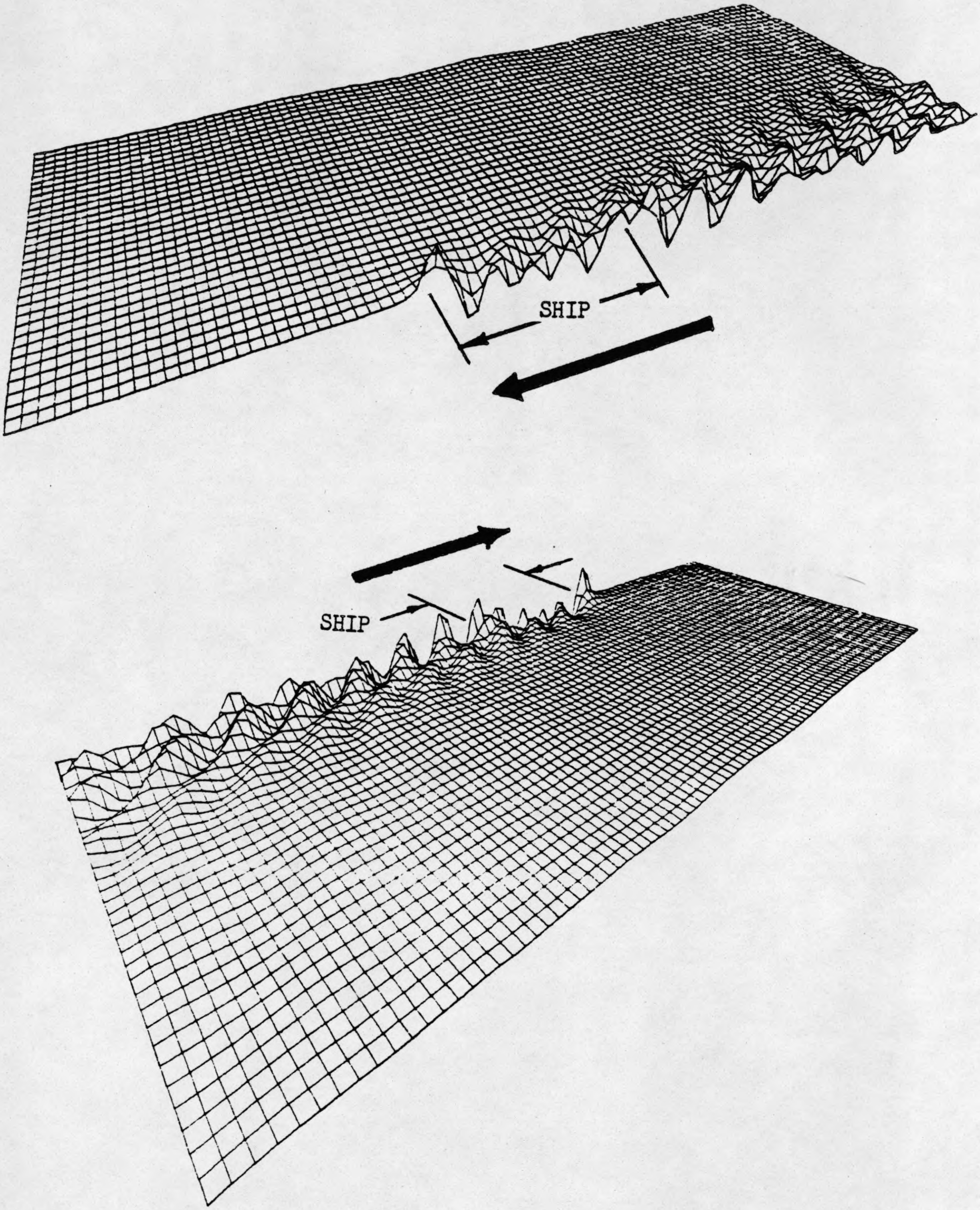

Figure 2.9e Two views of the free surface waves at T=5 for Fr=0.200.

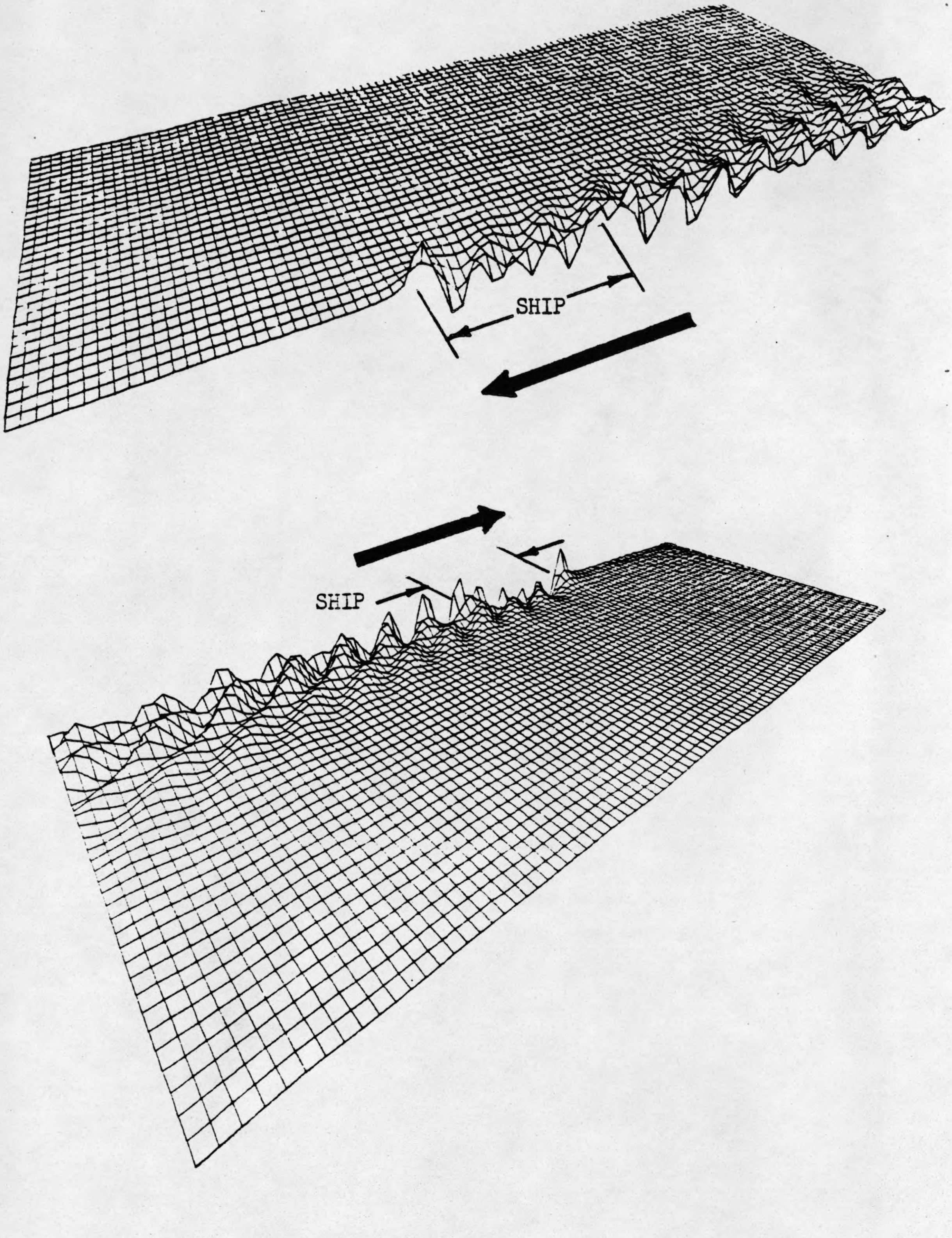

Figure 2.9f Two views of the free surface waves at T=6 for Fr=0.200.

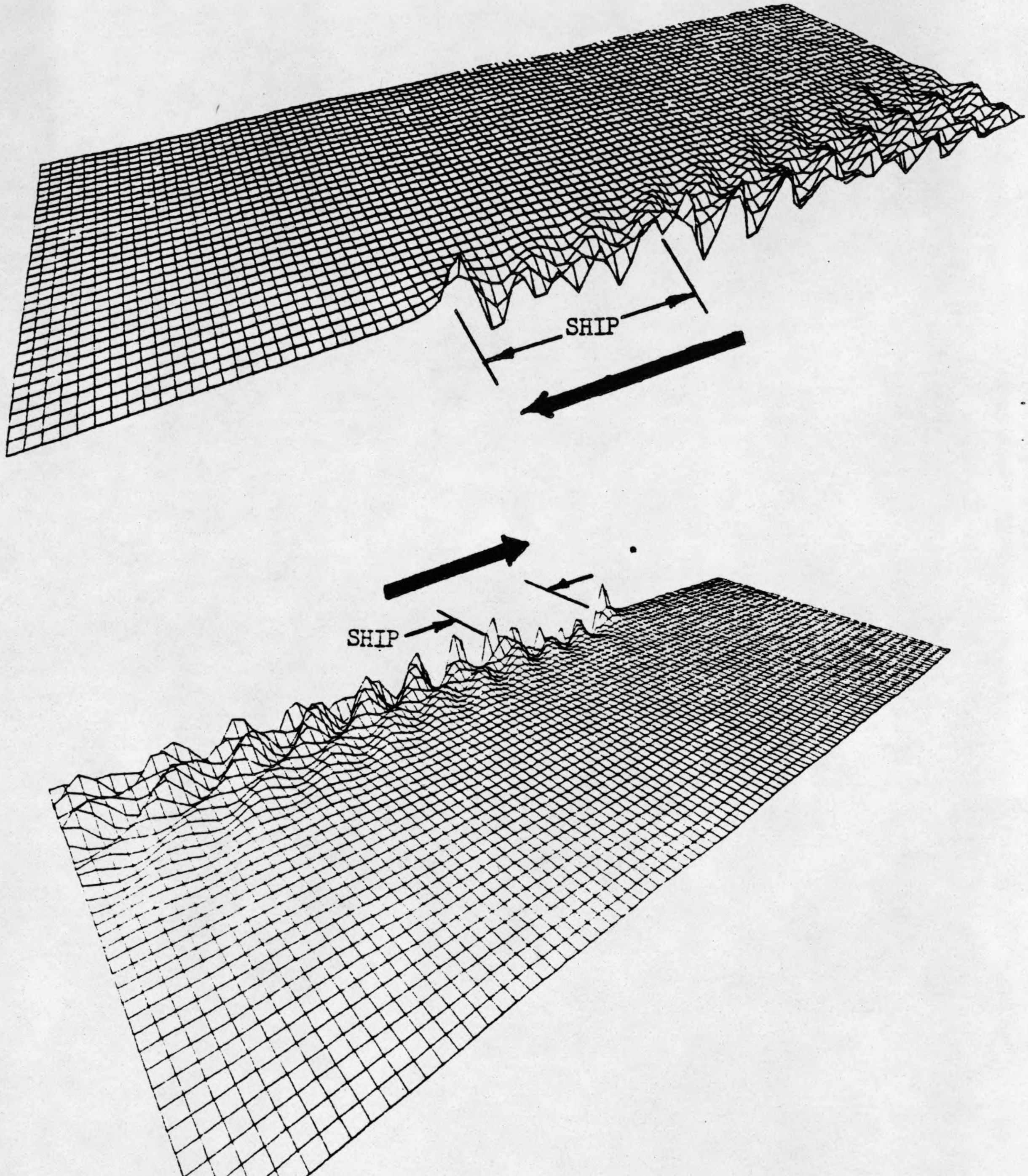

Figure 2.9g Two views of the free surface waves at T=7 for Fr=0.200.

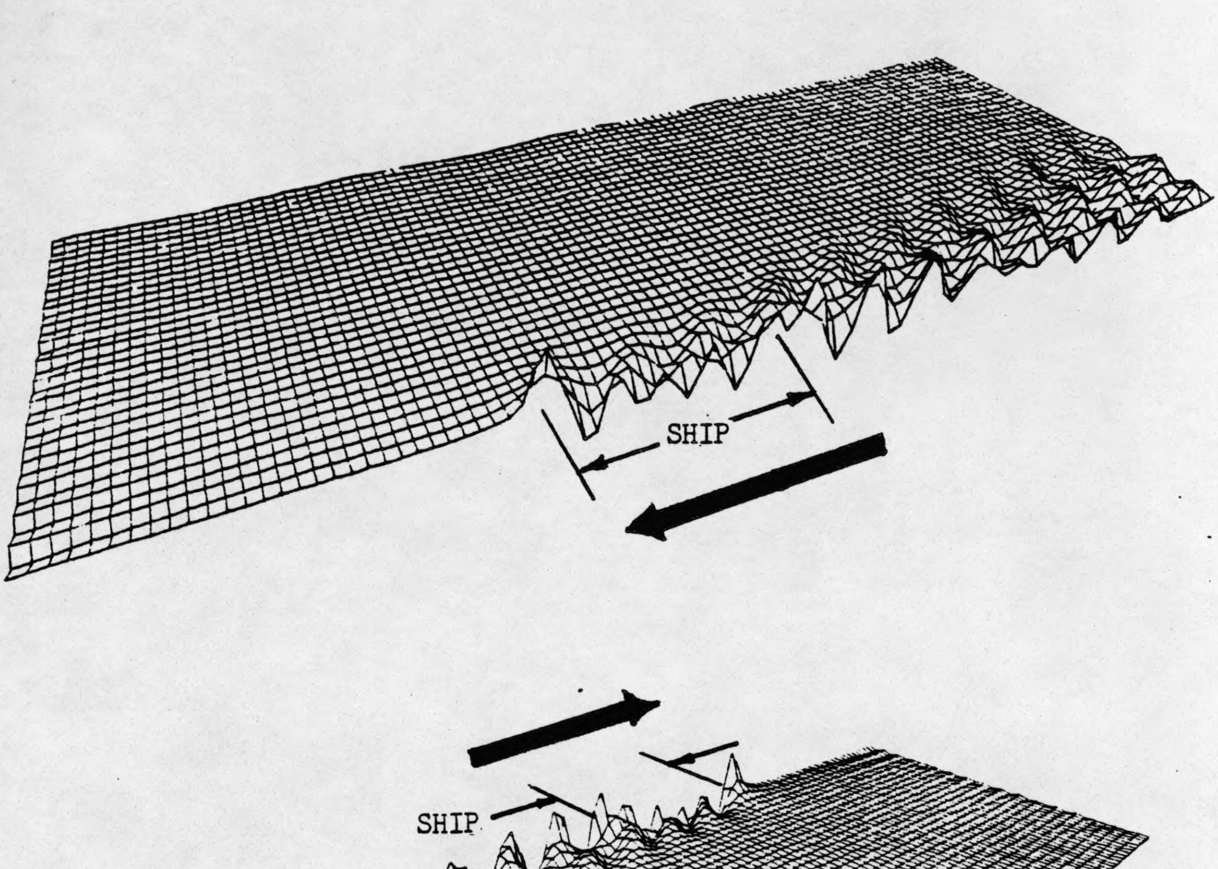

Figure 2.9h Two views of the free surface waves at T=8 for Fr=0.200. Two grid interval wave disturbances are seen to grow at the upstream corner near the symmetry plane.

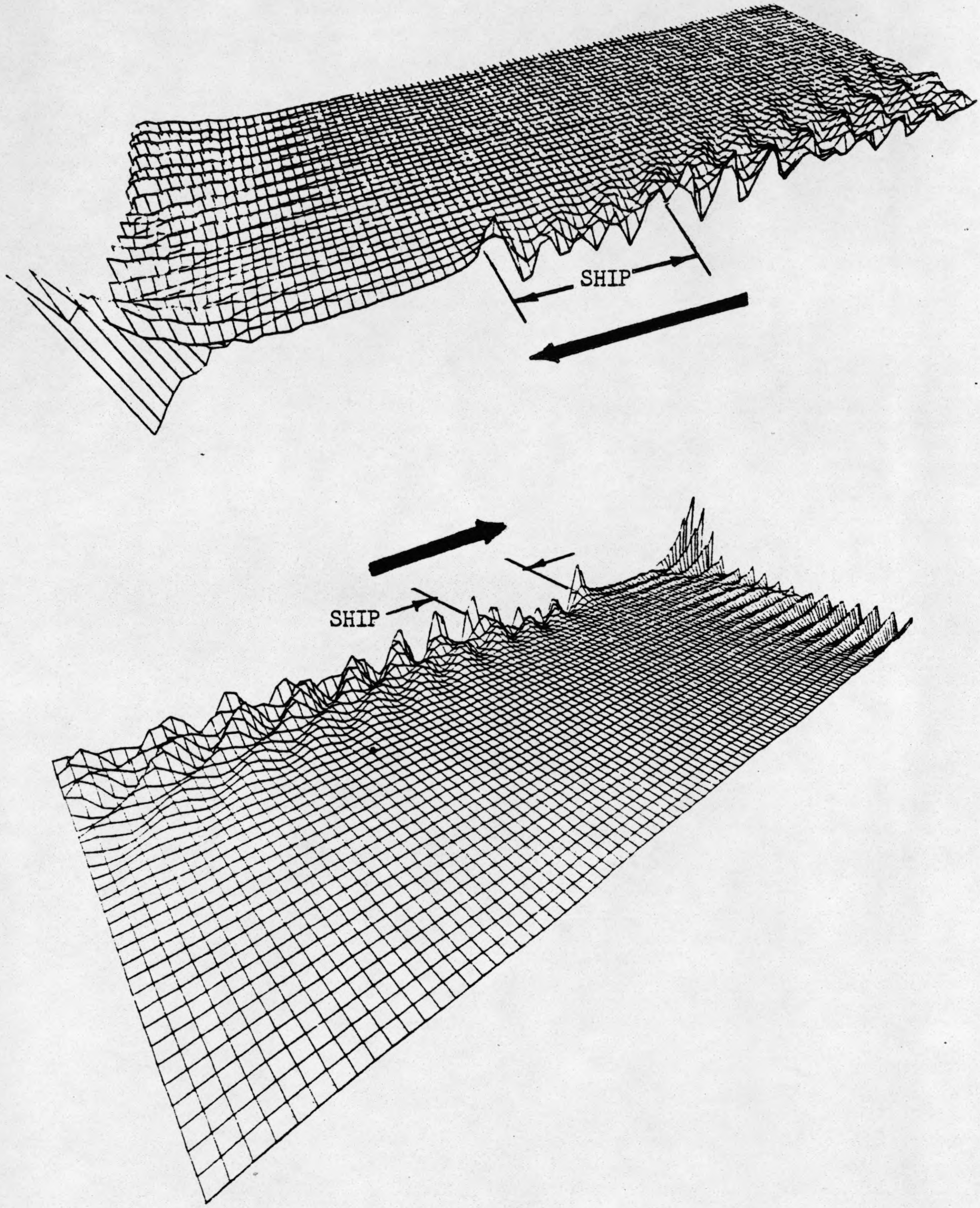

Figure 2.9i Two views of the free surface waves at T=9 for Fr=0.200. Two grid interval wave disturbances are seen to propogate downstream.

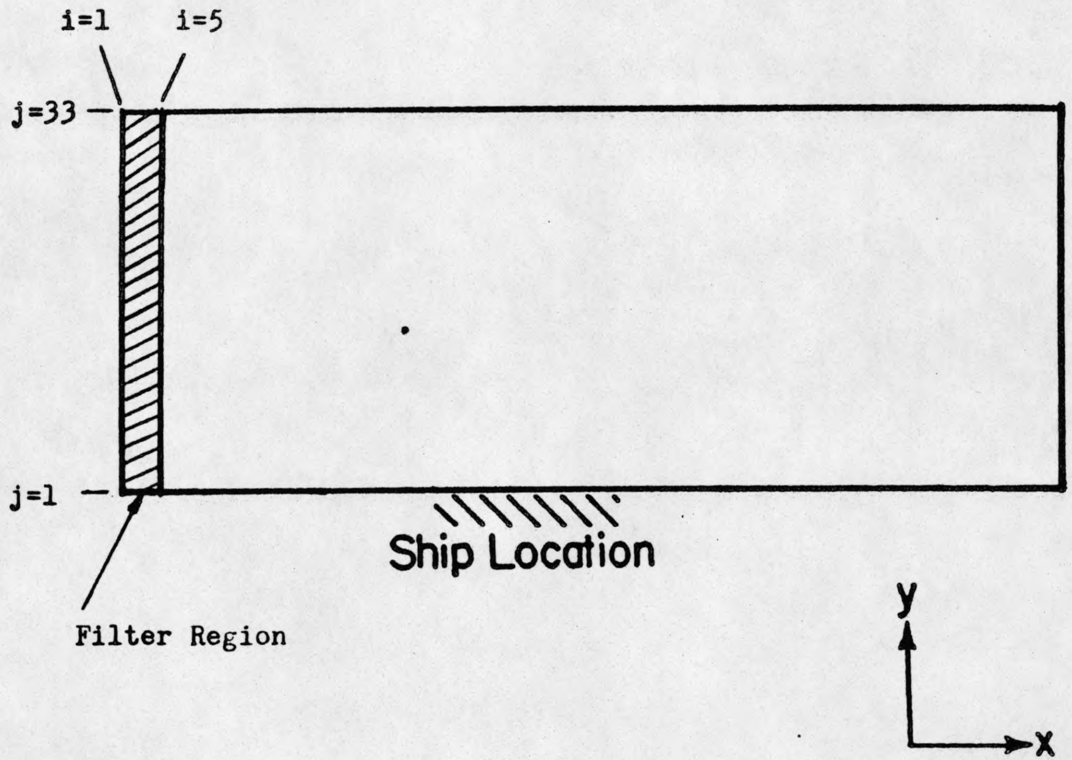

Figure 2.10 Illustration of the region where filtering is applied on the free surface every time step.

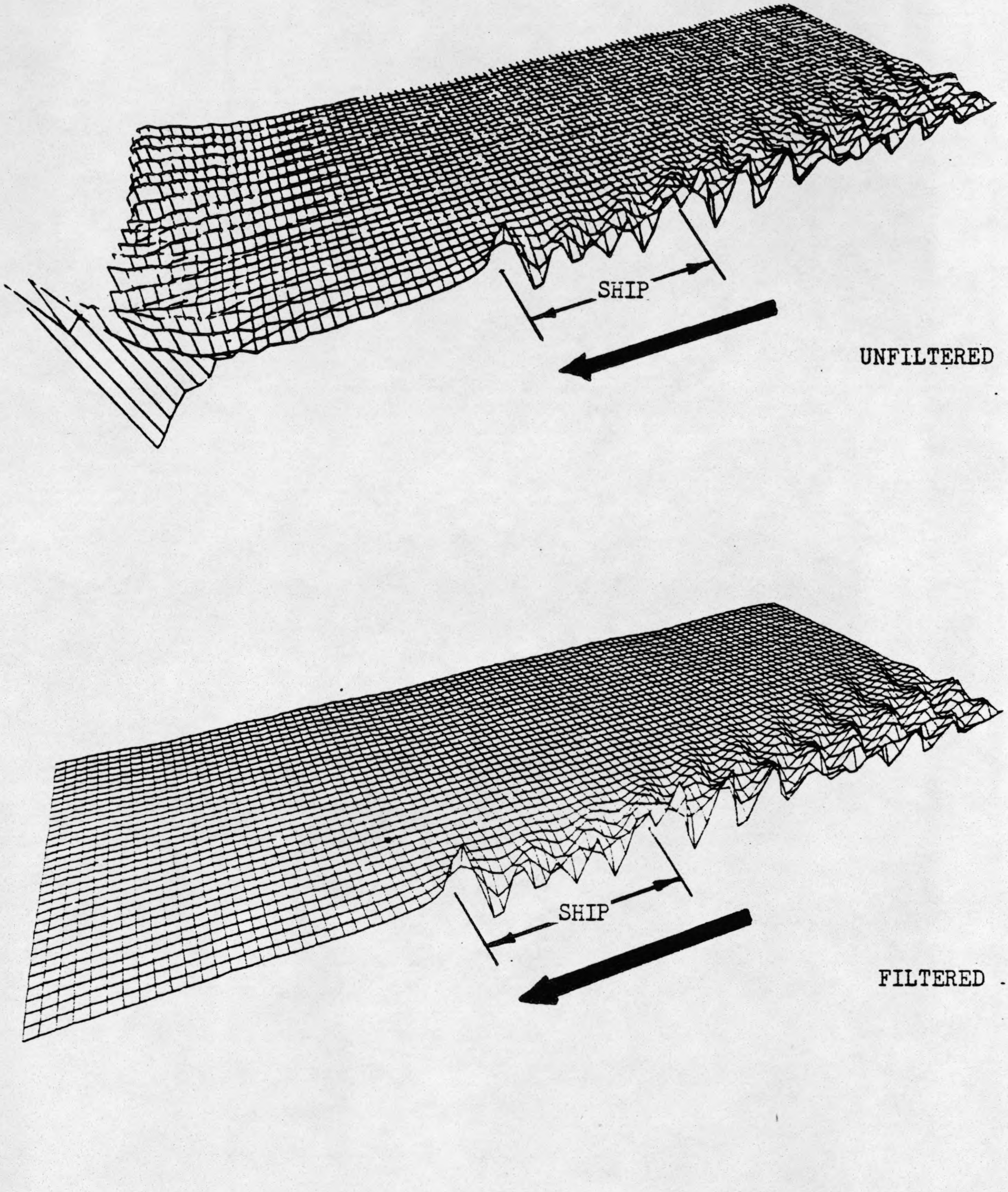

Figure 2.11 Views of the free surface waves for the unfiltered and the filtered cases at T=9 for Fr=0.200.

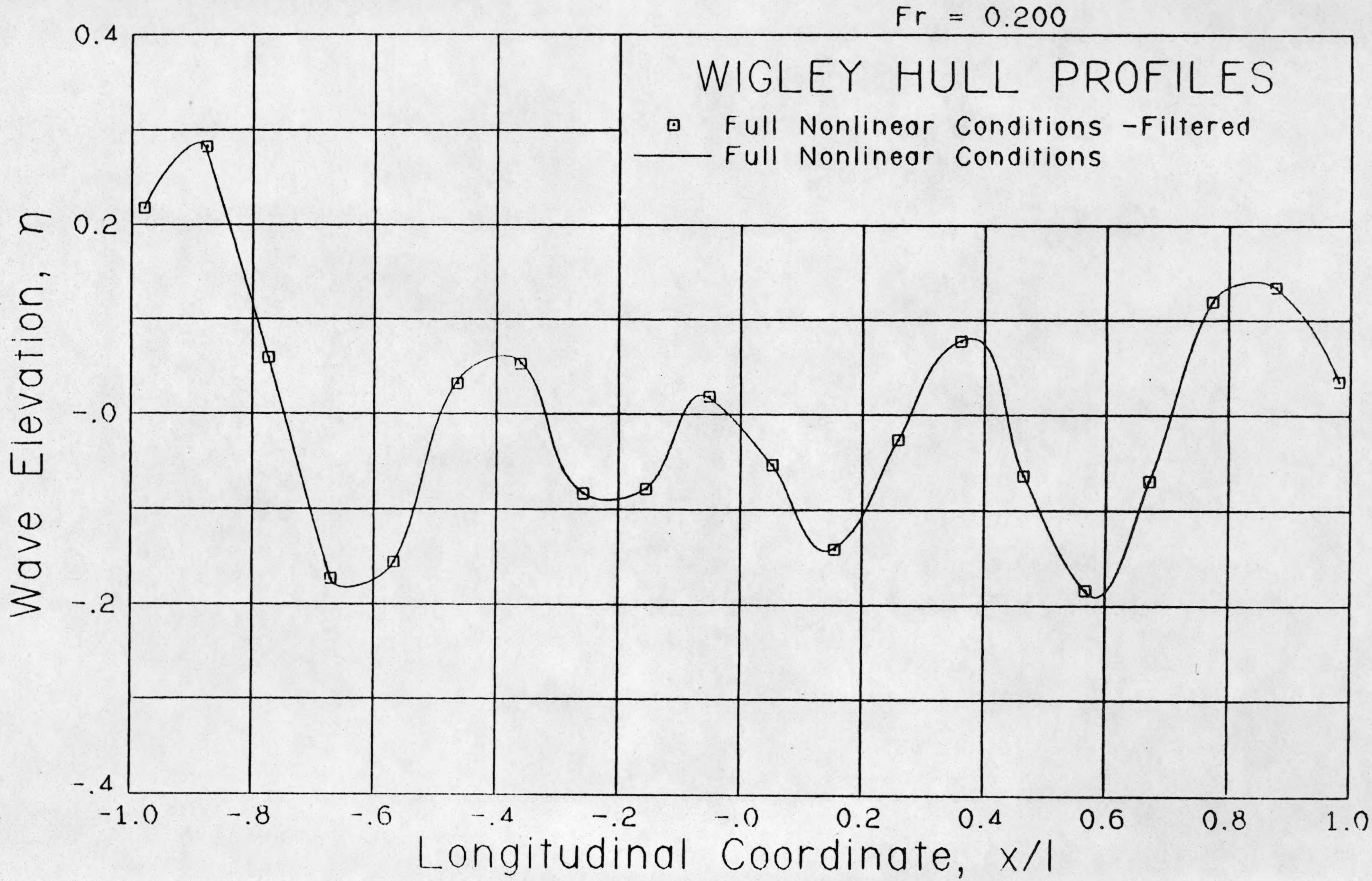

Figure 2.12 Comparison of the Wigley hull wave profiles for the filtered and the unfiltered cases for Fr=0.200.

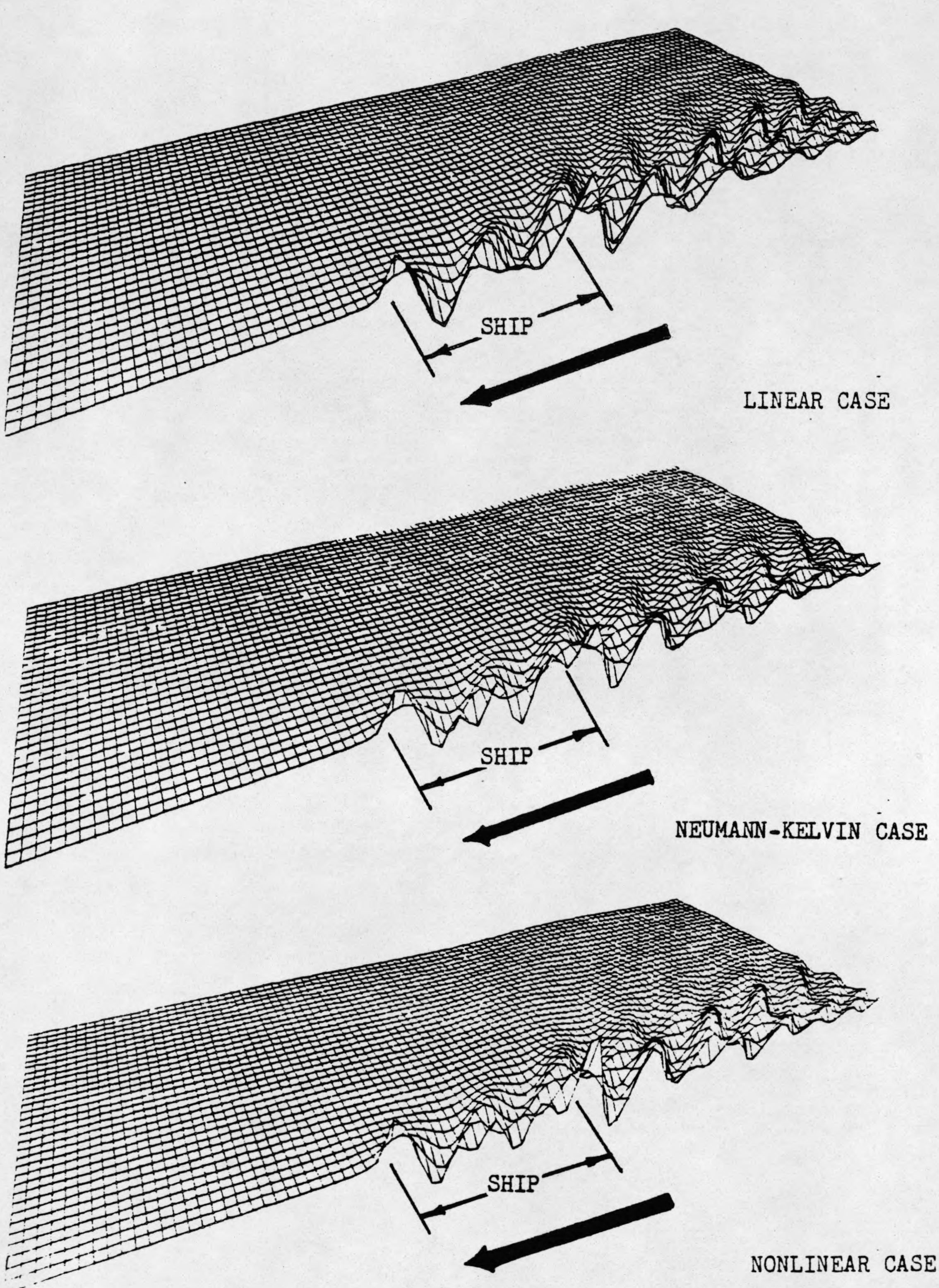

Figure 2.13a Views of the free surface waves for the linear, the exact hull and the nonlinear cases at T=3 for Fr= 0.266.

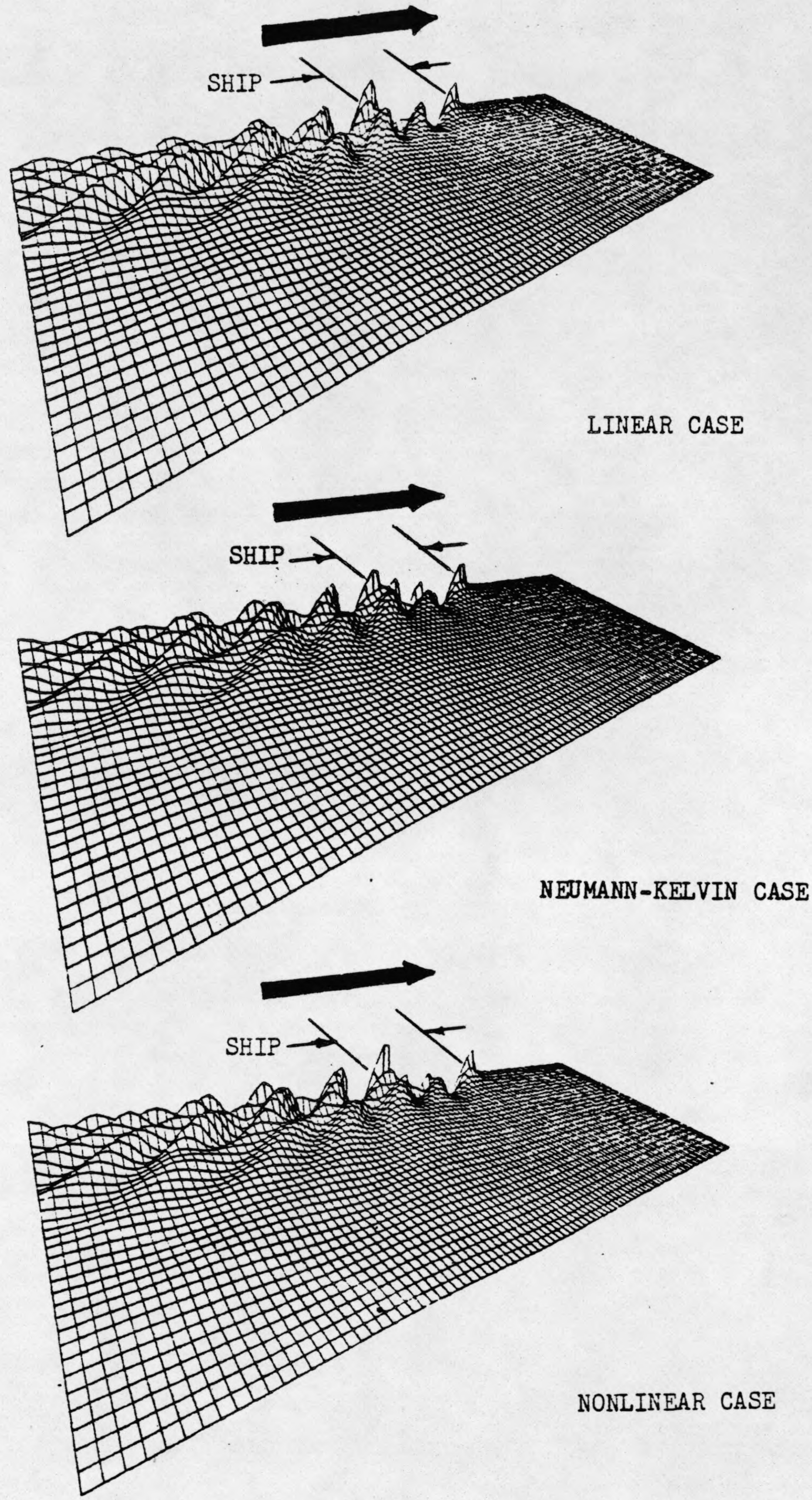

Figure 2.13b Views of the free surface waves for the linear, the exact hull and the nonlinear cases at T=3 for Fr= 0.266.

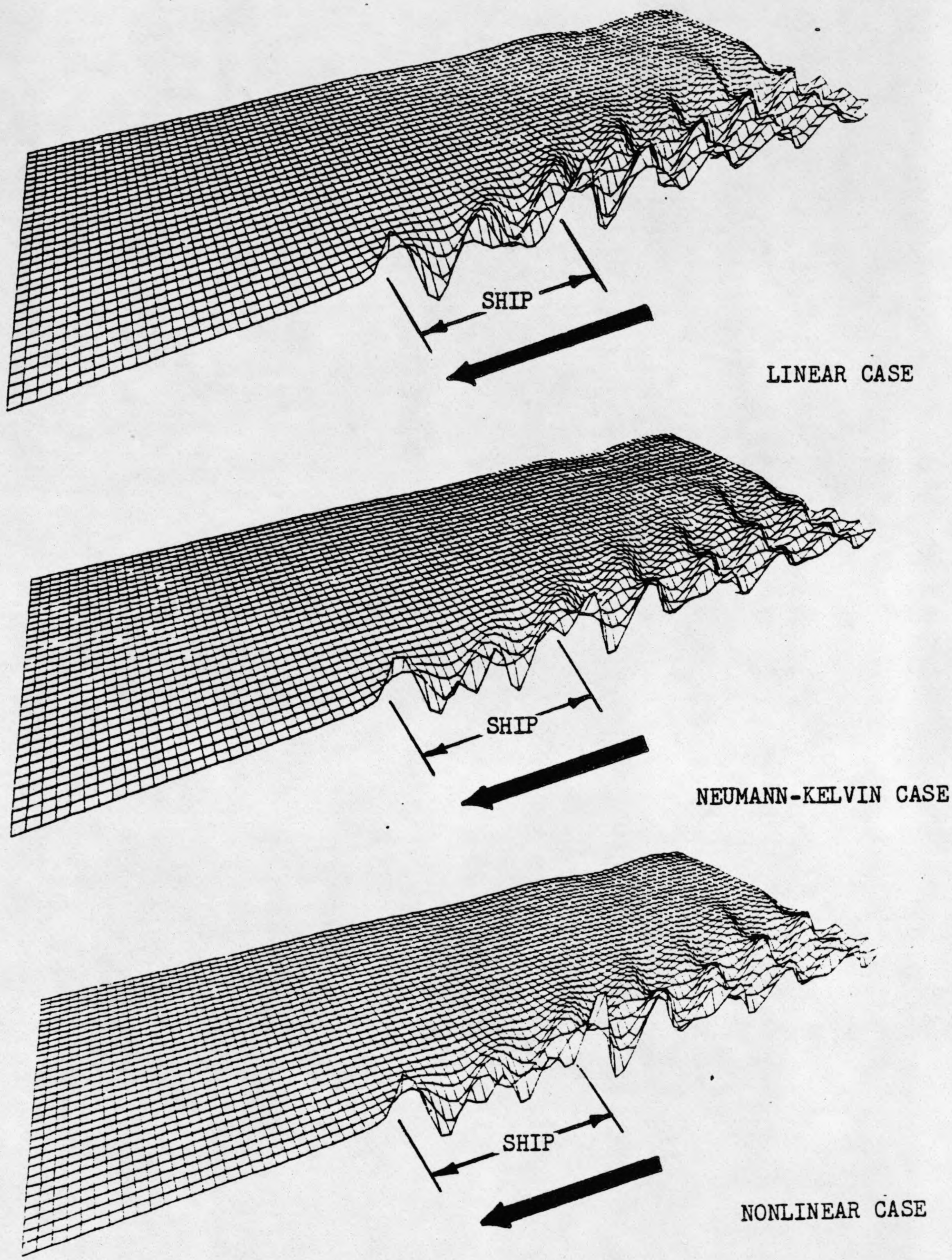

Figure 2.14a Views of the free surface waves for the linear, the exact hull and the nonlinear cases at T=6 for Fr= 0.266.

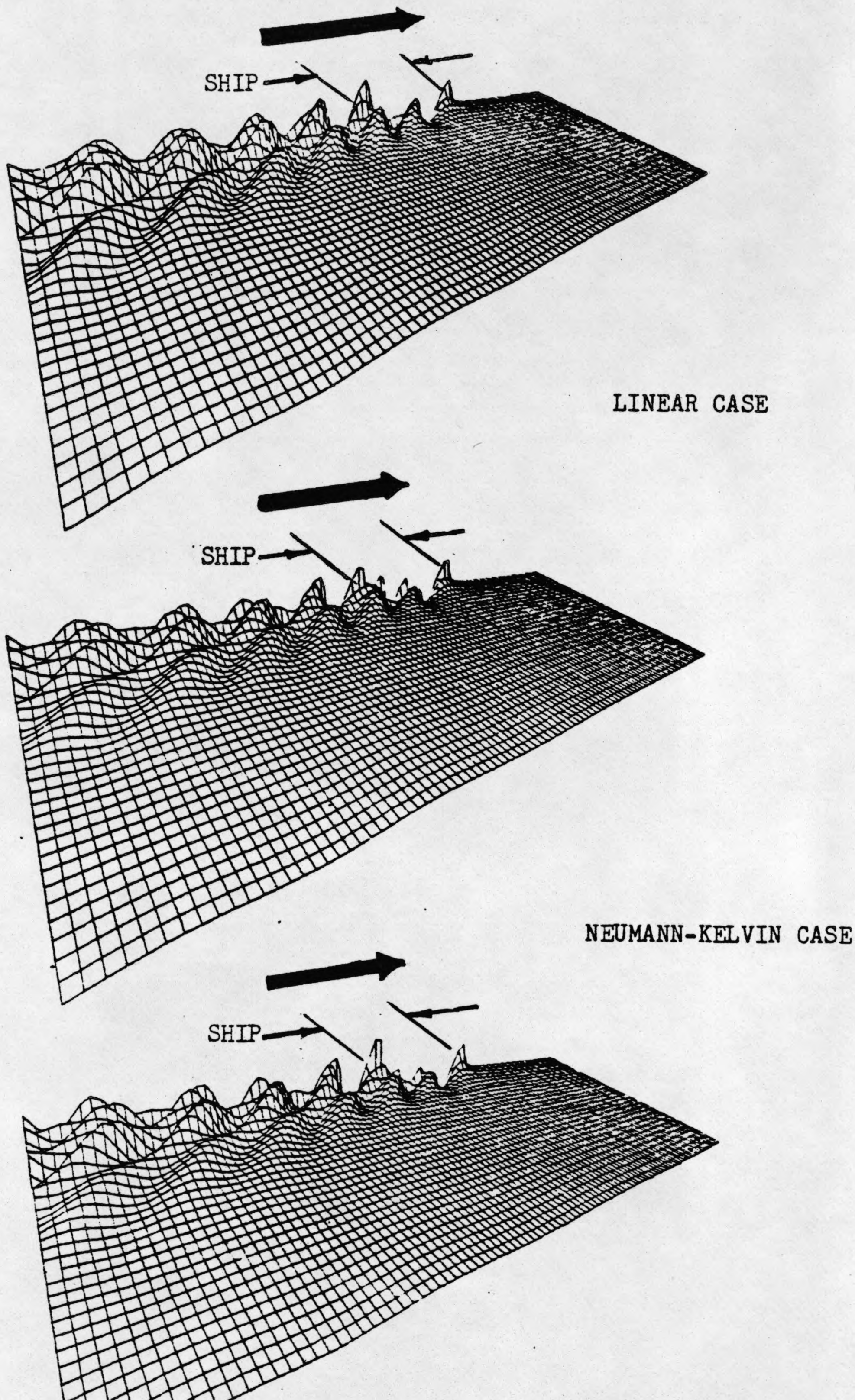

Figure 2.14b Views of the free surface waves for the linear, the exact hull and the nonlinear cases at T=6 for Fr= 0.266.

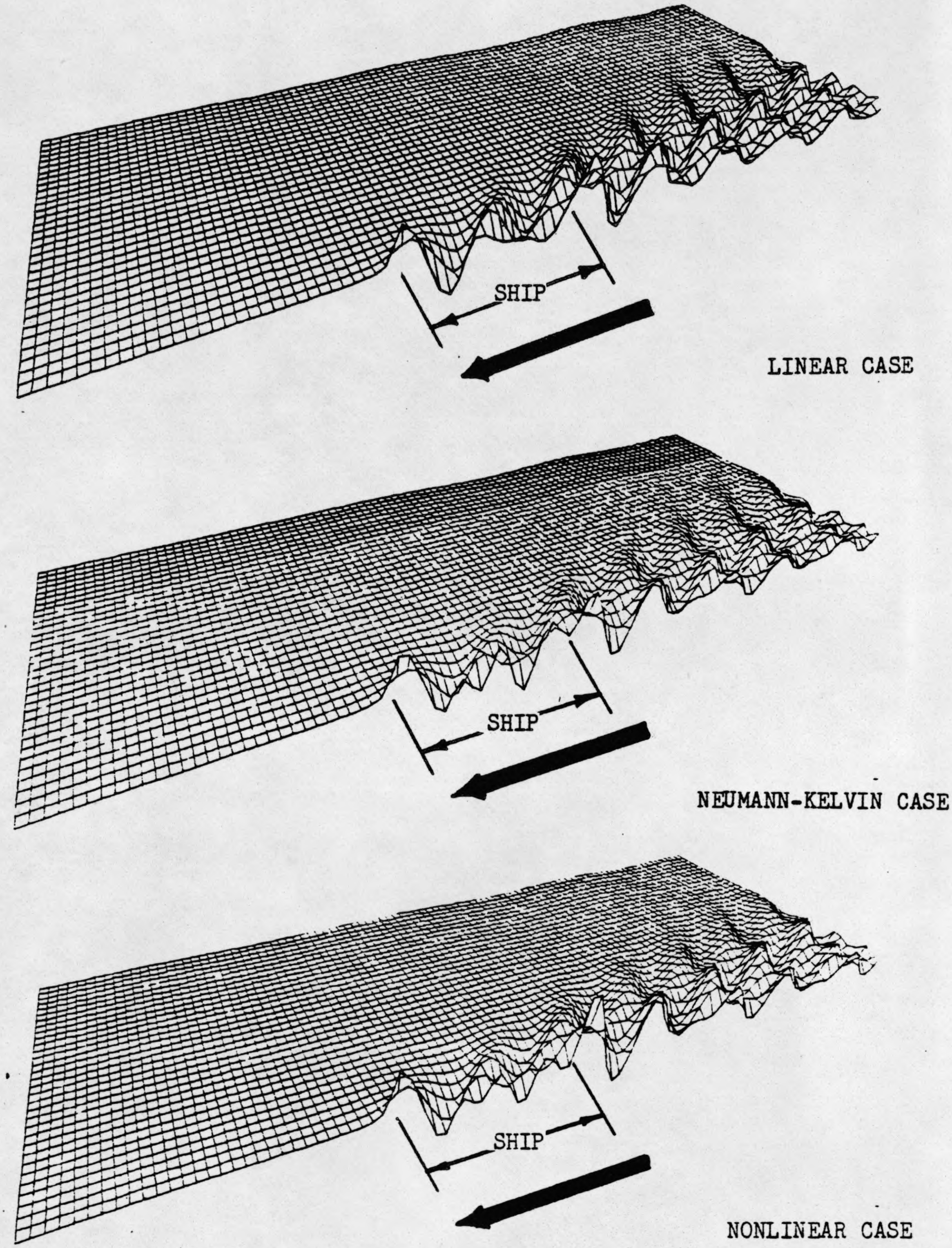

Figure 2.15a Views of the free surface waves for the linear, the exact hull and the nonlinear cases at T=9 for Fr= 0.266.

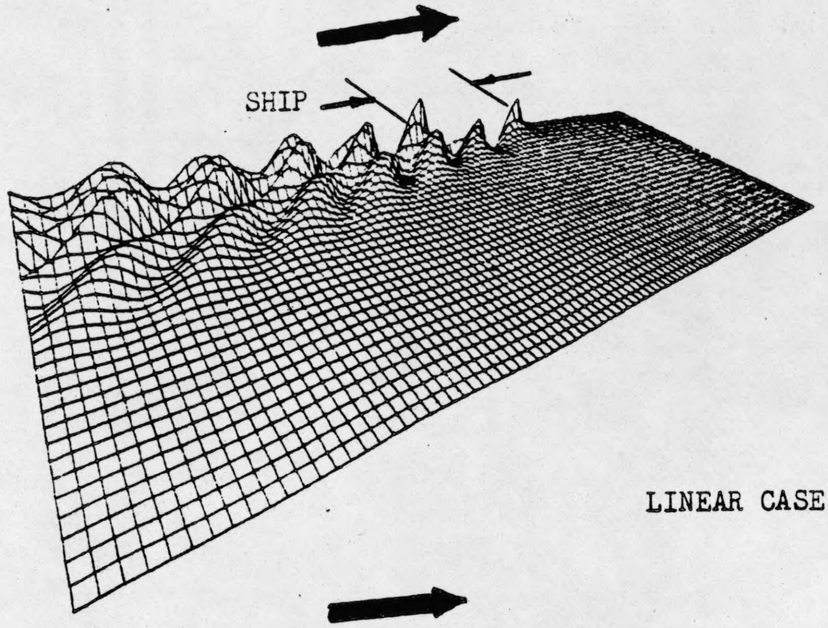

LINEAR CASE

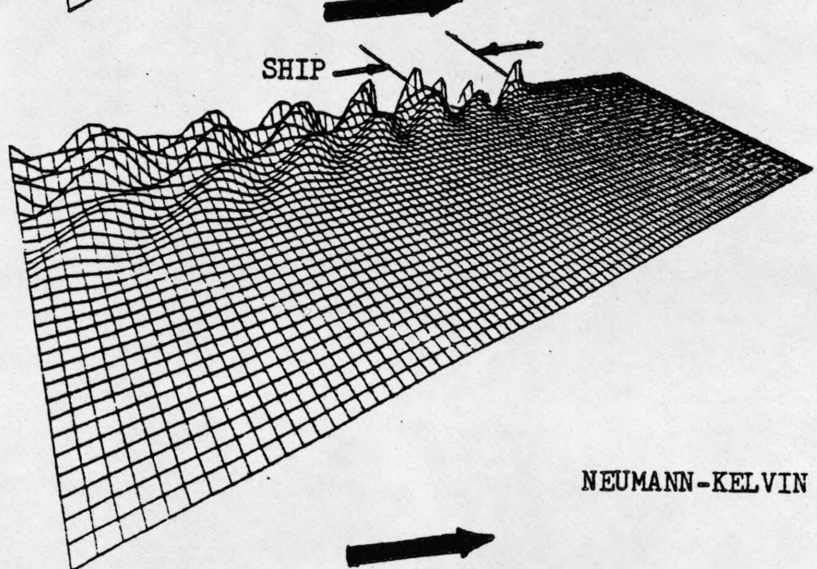

NEUMANN-KELVIN CASE

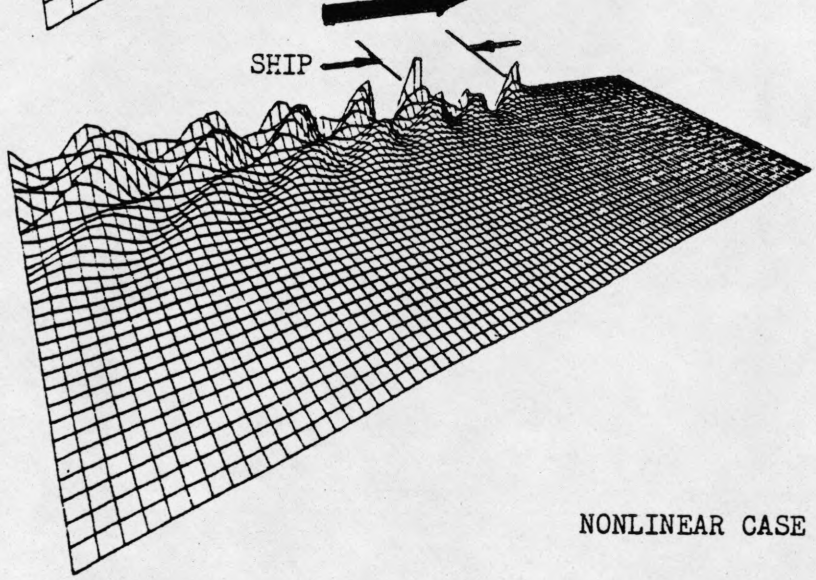

NONLINEAR CASE

Figure 2.15b Views of the free surface waves for the linear, the exact hull and the nonlinear cases at T=9 for Fr= 0.266.

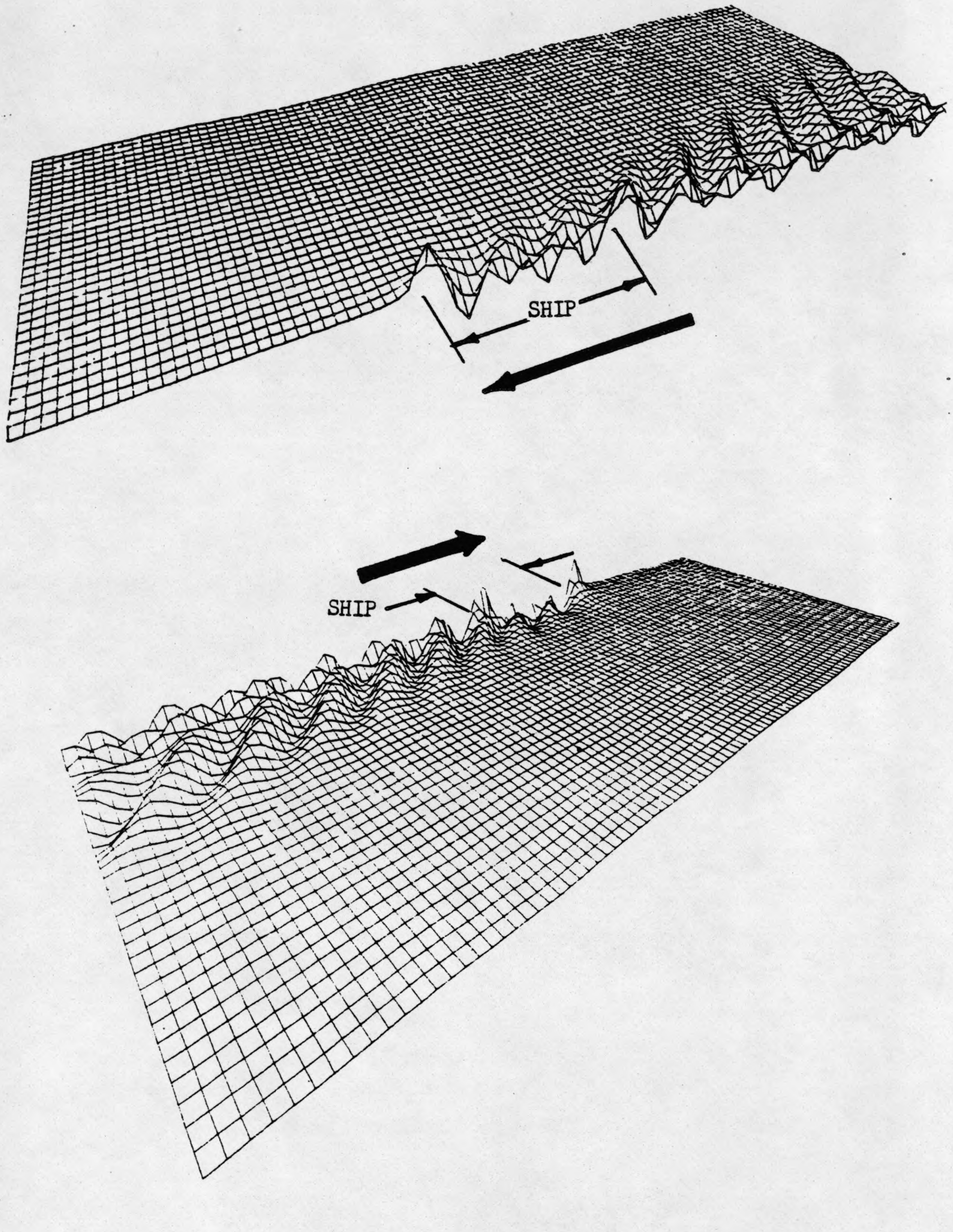

Figure 2.16 Two views of the free surface waves at T=9 for Fr=0.224.

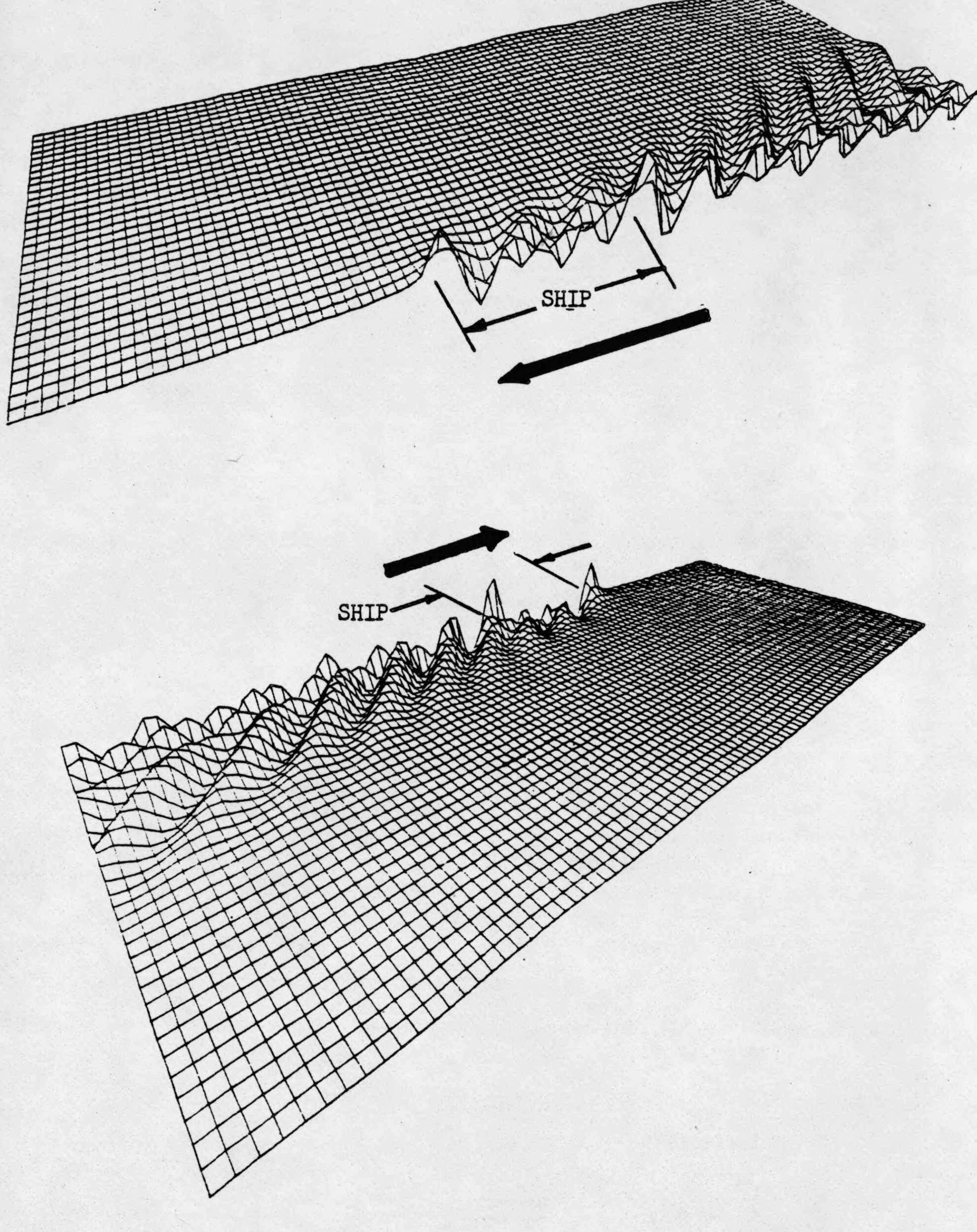

Figure 2.17 Two views of the free surface waves at T=9 for Fr=0.233.

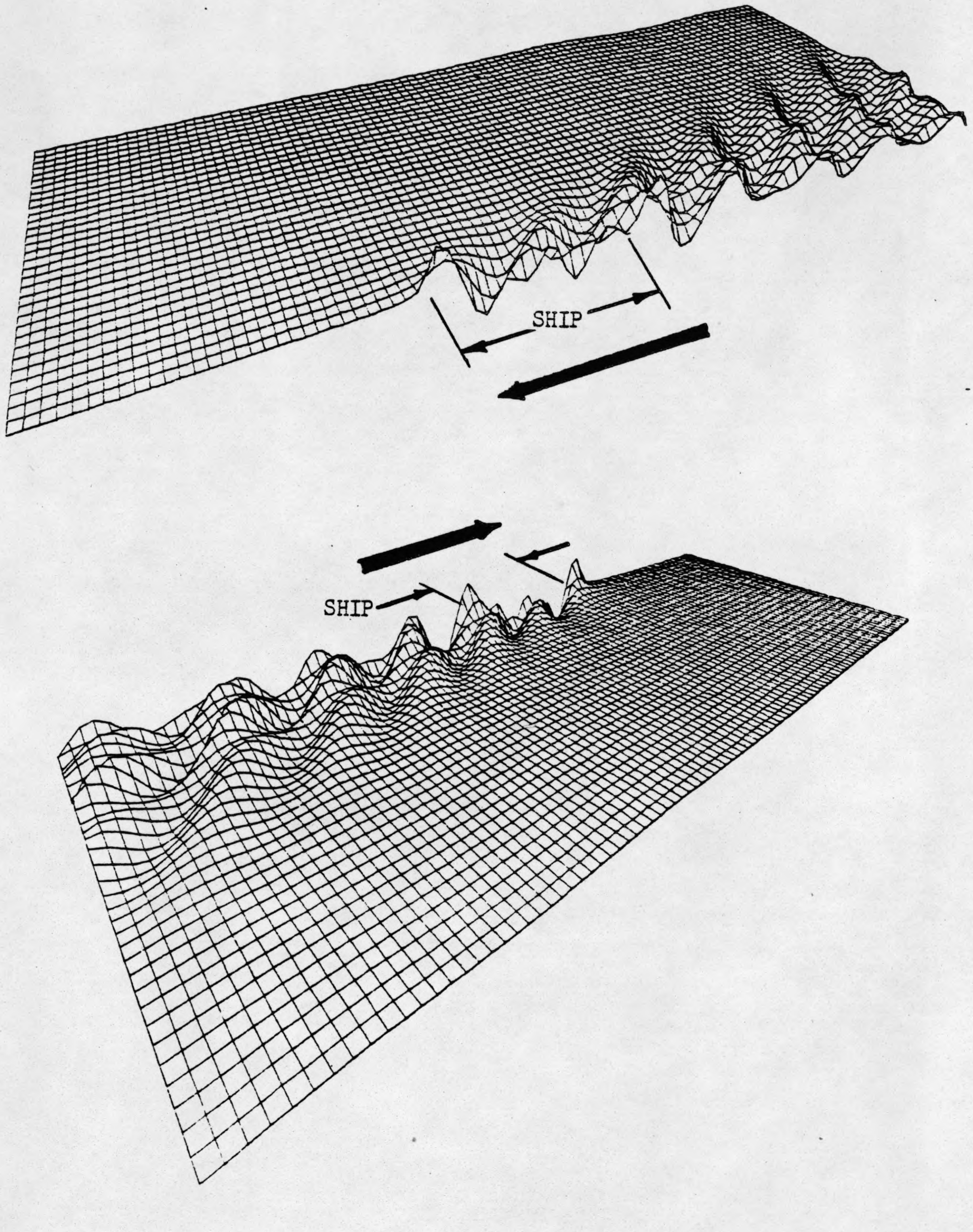

Figure 2.18 Two views of the free surface waves at T=9 for Fr=0.280.

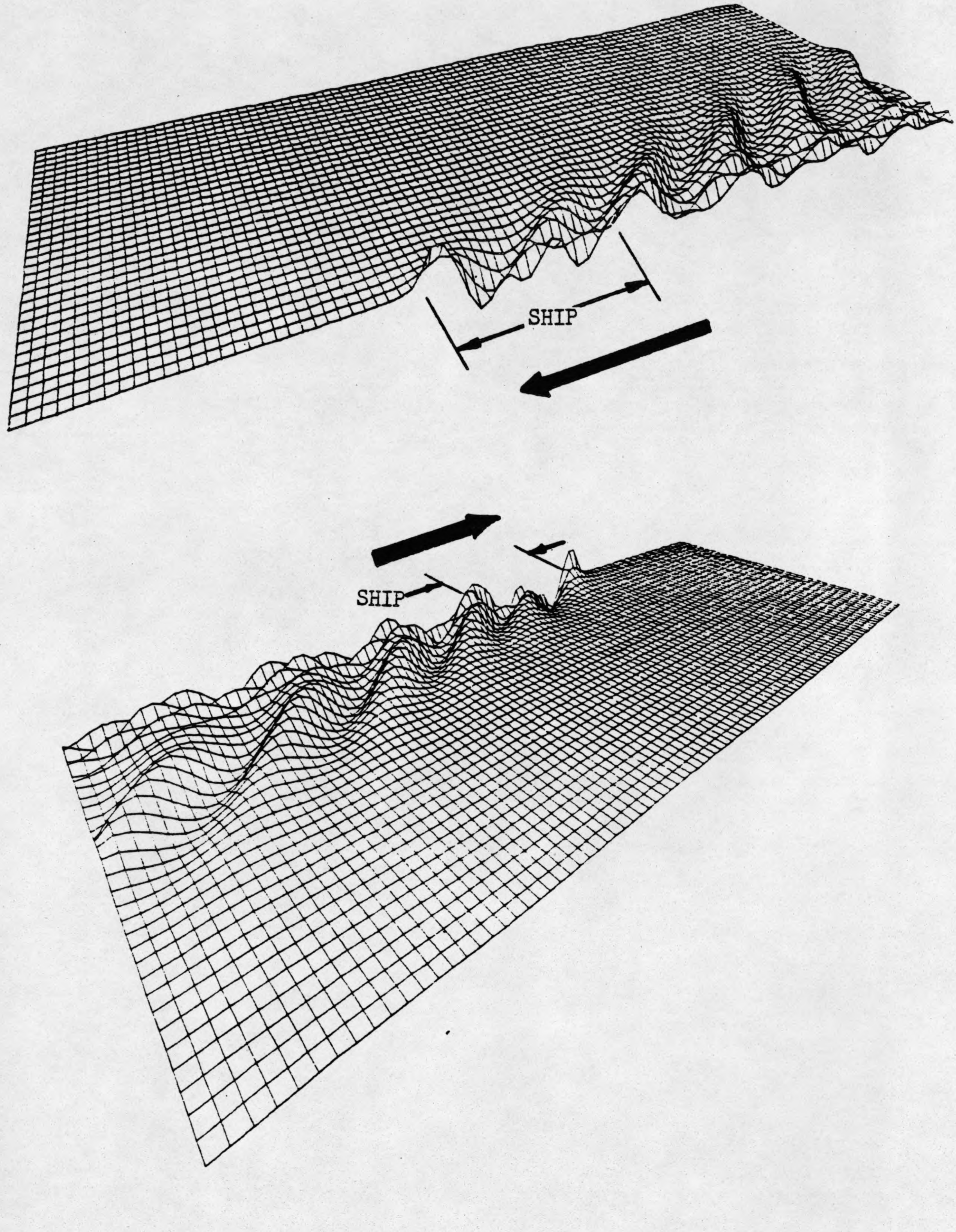

Figure 2.19 Two views of the free surface waves at T=9 for Fr=0.308.

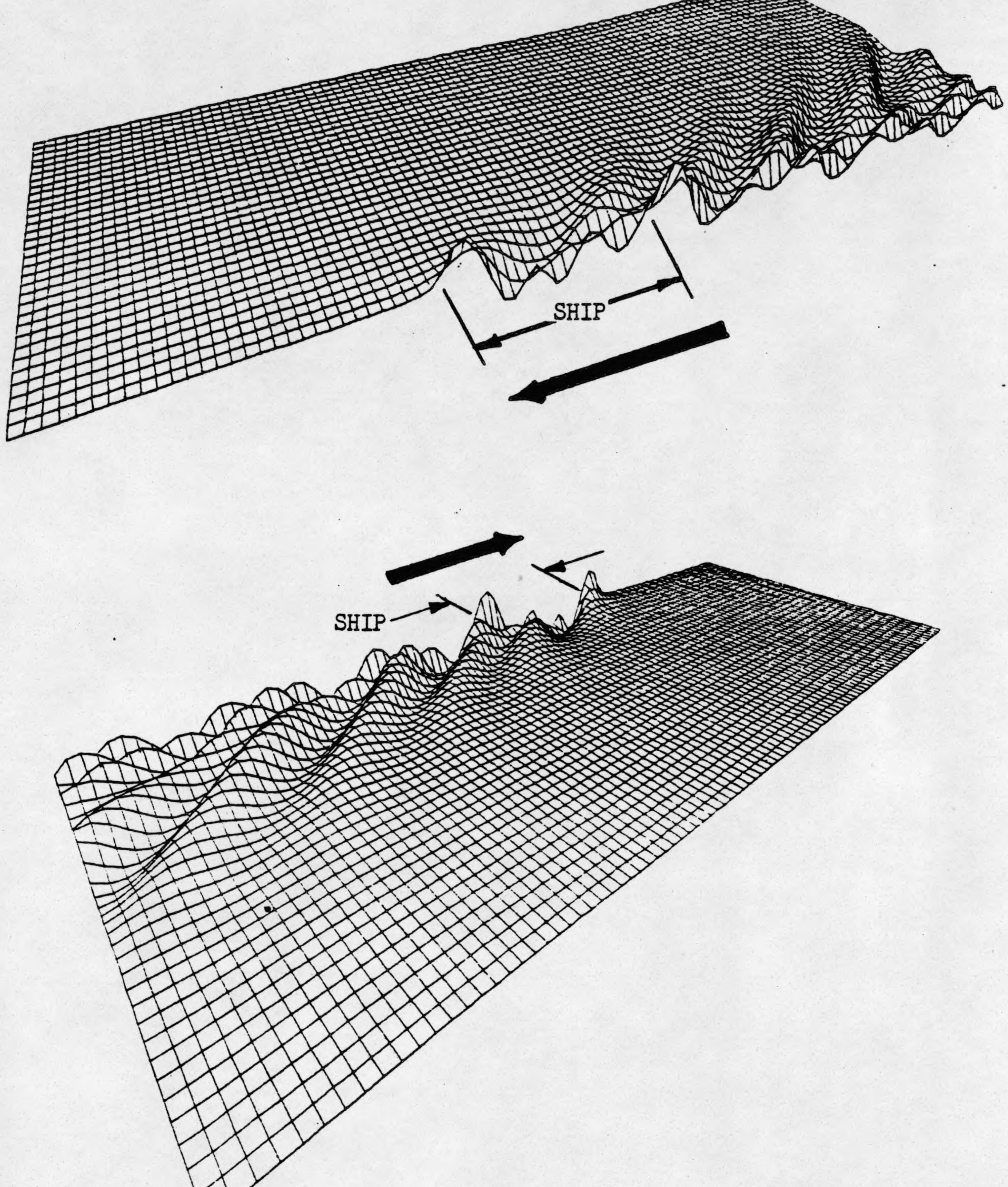

Figure 2.20 Two views of the free surface waves at T=9 for Fr=0.329.